ADDIS ABABA UNIVERSTY

ADDIS ABABA INSTITUTE OF TECHNOLOGY

SCHOOL OF GRADUATE STUDIES

INVESTIGATION ON POSSIBLE APPLICATION OF MAGNETORHEOLOGICAL BRAKE FOR LIGHT RAIL VEHICLE

A thesis Submitted to Mechanical Engineering in Partial Fulfillment of the Requirement for the Degree of Masters of Science in Mechanical Engineering (Rail way engineering Stream)

BY: Zekaryis Moges

ADVISOR: Dr.Ing Demiss Aleme

May 2015

ADDIS ABABA UNIVERSITY

SCHOOL OF GRADUATE STUDIES

A thesis Submitted to Mechanical Engineering in Partial Fulfillment of the Requirement for the Degree of Masters of Science in Mechanical Engineering (Rail way engineering Stream)

BY: Zekaryis Moges

ADVISOR: Dr.Ing Demiss Aleme

May 2015

DECLARATION

I, the undersigned, declare that this thesis is my original work and has not been presented for any degree in any university and all the sources of materials used for the thesis have been duly acknowledged.

Zekaryis Moges		21/05/2015
Name	**Signature**	**Date**

May 2015

APPROVAL SHEET

Approved by Board of Examining:

1. Dr.Ing Demiss Alemu **Advisor**		**Signature**	21/05/2015 **Date**
2. Fasil Gesesew **Internal Evaluator**		**Signature**	21/05/2015 **Date**
3. Haileleul Sahle **External Evaluator**		**Signature**	May 25, 2015 **Date**
4. Dr.Birhanu Beshah **Rail way center head**	Birhanu Beshah(PhD) Head,Railway Engineering Centre	**Signature**	25/05/15 **Date**

Director of Postgraduate Program
Addis Ababa University
Addis Ababa Institute of Technology

ACKNOWLEDGEMENTS

First of all, I am very glad to praise the Almighty God who has enabled me complete this study.

I am grateful for the support and supervision given by Dr.ing. Demis Alemu. He has shared his knowledge and never-ending ideology with me and is acknowledged for having made this year so rewarding. He has challenged me when I needed it, and encouraged me when I needed it, always being genuinely helpful and constructive. Thank you.

I convey my sincere thanks to Mr. Kebede for providing me the necessary materials during the course of my study and to perform this research.

I express my cordial gratitude to my parents for their unlimited support. I know that there is no way to repay my debt except make them proud of me.

I am grateful for having had great colleagues at my side. Writing MSc thesis is at times a lonesome and uncertain journey and it is of great importance to have supportive and friendly colleagues. I started as MSc student at the same time as Fesum. Having gone through this process in parallel, Fesum has been a great friend. The hardships have been easier to handle and the accomplishments have become more enjoyable thanks to him.

Finally I want to thank my classmate students and instructors at the department. To interact with ambitious, curious and bright people like you has been a fantastic experience that I will remember.

Zekaryis Moges

Addis Ababa

May 2015

ABSTRACT

Conventional pneumatic brake systems used in light rail vehicle have several limitations and disadvantages such as the response delay in building up the pressure necessary to actuate the brakes there is also, the long time delay between front and rear car, wear of braking pad and requirement for auxiliary components (e.g. compressor, transfer pipes, auxiliary reservoir and main reservoir) increase the overall weight and it is bulky in size of braking system. This paper presents an electromechanical brake system for light rail vehicle using magnetorheological (MR) fluid.

The proposed MR brake consists of rotating disks immersed into an MR fluid and an enclosed electromagnet. When current is applied to the electromagnet coil, the MR fluid solidifies as its yield stress varies as a function of the magnetic field applied by the electromagnet. This controllable yield stress produces shear friction on the rotating disks, generating a retarding braking torque. This type of braking system has the following advantages: faster response, easy implementation of a new controller or existing controllers (e.g. ABS etc.), less maintenance requirements since there is no material wear and lighter overall weight since it does not require the auxiliary components.

In this paper practical design criteria such as material selection and MR fluid selection are considered to select a basic MR brake configuration. The mechanical part is modeled using Bingham's equation, an approach to modeling the magnetic circuit is also proposed in this work. The equation of the torque transmitted by the MR fluid within the brake is derived, based on this equation, after mathematical manipulation, the torque generating by the MRB is investigated theoretically. The MRB in a rail vehicle was studied using a 1/8th vehicle model. Then, a finite element analysis is performed to investigate the resulting structural and heat distribution within the MR brake configuration.

Results shows that MRB generates much lower braking torque compared to that of braking torque required for train to stop and a finite element analysis results shows operating temperature can intermittently reach outside the recommended temperature range of the MR fluid, however possible design improvements are suggested to further increase the braking torque capacity and to reduce temperature rise.

TABLE OF CONTENTS

APPROVAL SHEET ..... **Error! Bookmark not defined.**

ACKNOWLEDGEMENTS iii

ABSTRACT iv

LIST OF FIGURES viii

LIST OF TABLES viii

NOMENCLATURE ix

LIST OF ACRONYMS xii

1. PROBLEMS AND ITS APPROACH 1

1.1 Background of the study 1

1.2 Statement of the Problem 3

1.3 Objectives of the Study 3

1.3.1 General objectives 3

1.3.2 Specific objectives 3

1.4 Methodology 4

1.4.1 Data and data source 4

1.4.2 Method of analysis 4

1.4.3 Research method 5

1.5 Scope 5

1.6 Limitation 5

1.7 Significance of the research 6

1.8 Research Outline 6

CHAPTER TWO 8

2. REVIEW OF LITERATURE 8

CHAPTER THREE 17

3. DYNAMIC MODEL OF A LIGHT RAIL VEHICLE 17

3.1. Kinematics equation of braking 17
3.2 Loading Capacity/Carrying Capacity of train 19
3.2.1 Train Weight 19
3.3 Kinetics of braking 20
CHAPTER FOUR 25
4. MODELING OF MR BRAKE 25
4.1 Properties of MR Fluids 25
4.2 Mathematical analysis of magnetorheological brake modeling 26
CHAPTER FIVE 30
5 DESIGN OF MR BRAKE 30
5.1 Conceptual Design 30
5.2 Material selection 30
5.2.1 Magnetic properties 30
5.2.2 Structural and thermal characteristics 32
5.3 MR fluid selection 33
5.4 Magnetic circuit design 34
5.4.1. Saturation flux density of selected materials 34
5.4.2. Mathematical analyses of magnetic circuit 36
5.5 Centrifugal force acting on MR brake 44
5.6 The maximum braking torque generated by MR brake 44
5.7 Thermal Analysis 46
5.7.1 Heat convection coefficient 47
5.8 MR brake 3D CAD modal 49
CHAPTER SIX 50
6 FINITE ELEMENT ANALYSIS 50
6.1 Introduction to Finite Element Analysis 50
6.2 Introduction to FEA Software ANSYS 51

6.2.1 General Analysis Procedure in ANSYS 51
6.3 Assumptions 51
6.4 Transient thermal analysis using ANSYS 14 52
6.4.1 Geometrical model 52
6.4.2 Definition of Material 53
6.4.3 Meshing 54
6.4.4 Definition of the loads and boundary conditions 55
6.5 Static structural analysis using ANSYS 14 56
6.5.1 Definition of the loads and boundary conditions 56
CHAPTER SEVEN 58
7 RESULTS AND DISCUSSIONS 58
7.1 Transient thermal Analysis Result 58
7.2 Static structural Analysis Result 59
7.2.1 Total deformation 59
7.1.2 Von Mises Stress 60
7.3 Braking torque generated by MR brake and braking torque required to stop rail vehicles 61
CHAPTER EIGHT 62
8 CONCLUSION AND RECOMMENDATION 62
9 REFERENCE 63
APPENDIX 65
Appendix A 65
Appendix B 66

LIST OF FIGURES

Figure 1 Cross section of an MRB actuator 10
Figure 2 Free body diagram of a wheel 20
Figure 3 Free body diagram of light rail vehicle body 22
Figure 4 MR Fluid model without outer magnetic field 25
Figure 5 MR Fluid model in outer magnetic field 26
Figure 6 Bingham's plastic model 26
Figure 7 Magnetorheological Brake modal 27
Figure 8 Magnetorheological fluids torque analytical diagram 28
Figure 9B-HCurve of steel 1018 for initial loading 32
Figure 10 B-H curves for MRF-241ES and MRF-132DG 33
Figure 11 Saturation point of low carbon steel, AISI 1018 35
Figure 12 Saturation points of MRF-132DG 36
Figure13 Magnetic circuit represent of MRB 37
Figure 14 Double disk type magnetorheological fluid magnetic circuit diagrams 39
Figure 15 Wire configurations in a coil 42
Figure 16: yield stress versus magnetic field intensity for MRF-132DG 43
Figure 17 shear disk analytical diagram 45
Figure 18 MR Brake 3D CAD modal: 49
Figure 19 Geometric Models of MRB 52
Figure 20 Meshed model of MRB 54
Figure 21 the loads and boundary conditions for thermal analysis 55
Figure 22 the loads and boundary conditions for structural analysis 57
Figure 23 Temperature gradients on MRB 58
Figure 24 Total deformations on the MR Brake 59
Figure 25 Von Mises Stress 60

LIST OF TABLES

Table 1 ER versus MR fluids 8
Table 2 Tramcar parameters were taken from Addis Ababa LRT project study report 17
Table 3 Loading capacity/carrying capacity of train 19
Table 4 Train Weight 19
Table 5 comparisons of the properties of ferromagnetic material B_m are values of the magnetic flux density at saturation μ_r are relative permeability values 31
Table 6 Properties of STEEL1018 32
Table 7 Properties of SS304 33
Table 8 properties of MRF-132DG 34
Table 9 Optimum design parameters 40
Table 10 Material Properties of AISI 1018 53
Table 11 Input data for transient thermal analysis 55
Table 12 input data for Structural analysis 56

NOMENCLATURE

v_f	Final velocity
v_o	Initial velocity
a	Deceleration during braking
S_b	Brake distance
t_b	Brake time
ω	The angular velocity of the wheel
α	Angular acceleration of wheel
W_t	The equivalent weight that the wheel carries
m_v	The mass of the vehicle
m_w	The mass of the wheel
W_{WS}	Weight on each wheel set in tones
V_{WS}	Velocity of the wheel set
T_b	Braking torque
F_r	The rolling resistances force
$F_{f,}$	The friction force
F_n	Normal force
F_L	The transfer of weight caused by braking of the vehicle
F_c	The centrifugal force
Ӫ	The angular acceleration of the vehicle
R_w	The radius of the wheel
I	The total mass moment of inertia
l_{base}	The wheel base
x	The distance traveled by the vehicle
η	The viscosity of the MR fluid with no applied magnetic field
γ	The shear rate.
τ	The total shear stress of MR fluids

τ_H	The yield stress developed in response to the applied magnetic field
N	The number of surfaces of the brake disk(s) in contact with the MR fluid
R_1	The outer radii of the shear disc
R_2	Inner radii of the shear disc
h	The thickness of the MR fluid gap
$\Re$	Reluctance
i	Current supplied to the electromagnet
I_{densty}	Current density
B_H	Saturation flux density of MRF-132DG
B_A	Saturation flux density of low carbon steel
H	The magnetic field intensity,
ϕ	The flux generated
H_{CORE}	Field intensity the magnet core
H_{DISK}	Field intensity of shear disk
H_{MRF}	Field intensity of shear disk
l_{CORE}	Length/thickness of magnet core
l_{DISK}	Length/thickness of shear disk
l_{MRF}	Length/thickness of the shear disk
T_η	Torque generated due to the viscosity of the fluid.
T_H	Torque generated due to the applied magnetic field
l	Length
μ_r	Relative permeability of material
μ_o	Vacuum's permeability
μ_{rMRF}	Relative permeability magnetorheological fluid
μ_{rA}	Relative permeability of low carbon steel
A	Cross-sectional area
Q	Heat energy developed

q	Heat flux
h_{cg}	The height of the center of gravity
h	Heat convection coefficient
K_{air}	Conductivity of air
V_{rail}	Railway speed
μ_{air}	Dynamic viscosity of air
C_{air}	Specific heat capacity of air

LIST OF ACRONYMS

MR Magnetorheological

MRB Magnetorheological Brake

MRF Magnetorheological Fluid

ERF Electrorheological fluid

DC Direct current

EMB Electro-Mechanical Brake

FEM Finite element model

MDO Multidisciplinary design optimization

KE Kinetic energy

mmf Magnetomotive force

CHAPTER ONE

1. PROBLEMS AND ITS APPROACH

1.1 Background of the study

The topic of "brake-by-wire" is a focus topic to automotive industries due to its potential to improve vehicle performance, safety and cost due to this reason billions of dollars are invested in research and development. The term "brake-by-wire" system is electronically controlled brake system this means that the mechanical connection between the brake actuator on each wheel set and the driver's brake valve handle replaces with electrical components that are able to do the same task in a faster, more reliable and better means of controlling braking processes in accurate way than the pure mechanical systems. This is a good case to increased performance and functionality of today's method of breaking system in a train [1] [2] [3] [4].

Using pure electronically controlled brake systems have many advantages. The properties and behavior of the brake will be easy to adapt by simply changing software parameters and electrical outputs instead of adjusting mechanical components. This also allows easier integration of existing and new control features such as anti-lock braking system (ABS), vehicle stability control (VSC), electronic parking brake (EPB), etc., as well as vehicle chassis control (VCC) and adaptive cruise control (ACC). The other advantages are the wiring will be simplified as less mechanical components are used, reduced wear out of wheels and rail due to more adaptive and economical brake functions, less mechanical/hydraulic/pneumatic components due to replacement of electronic parts, at the same time it will be possible to optimize maintenance intervals [1] [2] [3] [4].

The main contribution of this thesis is to development of a new brake-by-wire system for light rail vehicle application, using an electromechanical brake (EMB) that employs magnetorheological (MR) fluid. It consists of a rotating disk enclosed by a static casing and the gap between the disk and casing is filled with the MR fluid. A coil winding is embedded on the perimeter of the casing and when electrical current is applied to it, magnetic fields are generated, and the MR fluid in the gap becomes solid-like instantaneously. The shear friction between the rotating disk and the solidified MR fluid provides the required braking torque. In

principle, the brake torque can be controlled by changing the DC current applied to the electromagnet.

Magnetorheological fluids (MR) are a class of smart materials whose rheological properties (e.g. Viscosity) may be rapidly varied by applying a magnetic field. They are created by adding micron-sized iron particles to an appropriate carrier fluid such as oil, water or silicon. Their rheological behavior is almost the same as that of the carrier when no external magnetic field is present. However, when exposed to a magnetic field, the iron particles acquire a dipole moment aligned with the applied magnetic field to form linear chains parallel to the field. This reversibly changes the liquid to solid-like that has a controllable yield strength, which its magnitude depends directly on the magnitude of the applied magnetic field [1] [4].

Two important characteristics of MR fluids are:

(i) They exhibit linear response, i.e., the increase in stiffness is directly proportional to the strength of the applied magnetic field and

(ii) They provide fast response, i.e., MR fluid changes from a fluid state to a near-solid state within milliseconds of exposing a magnetic field [1].

Due to these unique characteristics nowadays, MRF is applicable include brakes, dampers, clutches and shock absorbers systems.

MRB is a friction based brake like conventional electro-pneumatic brake systems. However, the method of the friction generation in an MRB is entirely different. In the conventional electro-pneumatic brake systems, when the driver brake valve handle is placed on brake applied position, the stator and rotor surfaces come together and friction is generated between the two surfaces, resulting in the generation of the braking torque. But in the MRB, MRF is filled between the stator and the rotor, and due to controllable rheological characteristics of the MRF, shear friction is generated (thus the braking torque) [4].

1.2 Statement of the Problem

Conventional electro-pneumatic brake systems used in rail way cars have several limitations and disadvantages. First of all, when the driver's brake valve handle is placed on brake position, there is a response delay in building up the pressure necessary to actuate the brakes. There is also, the long time delay between front and rear car, since electro-pneumatic brake systems employ a highly pressurized brake fluid, there is the possibility of leakage of the brake fluid that would need extra energy to compensate leakage.

Another problem seen in conventional electro-pneumatic brake systems is that this type of brake uses the friction between brake pads and the brake disk as its braking mechanism, leading to the brake pad wear. Due to both the material wear and the friction coefficient variation in high speeds, the brake performs less optimally in high speed region, as well as with the increased number of usage cycles. Thus, the brake pads must be changed periodically in order to get the optimum braking performance. Hence, it involves a lot of mechanical system that is needed to be replaced or adjusted mechanically over a period of time or when necessary depend on driving behavior and rail condition. Finally, another limitation of this type of brake system is auxiliary components (e.g. compressor, transfer pipes, auxiliary reservoir and main reservoir) increase the overall weight and it is bulky in size of braking system.

1.3 Objectives of the Study

1.3.1 General objectives

The main objective of this study is to investigate the possibility of a magnetorheological brake for light rail vehicle application.

1.3.2 Specific objectives

The specific objectives of this study are:

- To develop the analytical model of magnetorheological brake.
- Select proper materials for magnetorheological brake (MRB) with adequate structural, thermal and magnetic properties.

- Design magnetic circuit of the magnetorheological brake (MRB) with considerations of torque generation.
- Compare torque required to stop the vehicles and torque generates by MRB.
- Generate a 3-D CAD model of magnetorheological brake.
- Creating an accurate structural and heat transfer finite element model (FEM) of the magnetorheological brake that simulates the braking behavior.

1.4 Methodology

1.4.1 Data and data source

The first thing to do for this study is evaluating the resources that are available by searching the primary and secondary data from ERC, documents and other scientific literature.

1.4.1.1 Method of data collection

The primary as well as secondary data which are needed for this study is collected using different data collection techniques. These are:

- By observing roots of the rail way to predetermine, what contaminants could exist?
- By consulting advisors and discussing with friends.
- Searching for thesis, publishing's, newspapers, books, etc. on different web sites which are helpful for meeting the general objective and the specific objective as well.

1.4.2 Method of analysis

After data is collected, analysis will be followed using different technique. These include:

- Creating possible strategies using words and simple diagrams
- Preparing the 3D model and will make analysis using simulation software called ANSYS.

1.4.3 Research method

I. First of all a lot of paper and journal will read up and a part of it will be considering in this project. Meanwhile, specifications and parameter value of light rail vehicle needed to calculate braking torque required to stop light rail vehicles and taken from LRT project specifications.

II. Next, the required braking torque to stop light rail vehicles are obtained, after properties of MR fluids explained and the behavior of MR fluid is modeled using the Bingham plastic model, finally the total braking torque generated is analytically described in terms of the magnetic field intensity applied and the viscosity of the fluid.

III. After that, material selection and MR fluid selection discussed then design the magnetic circuit after total braking torque generated which is analytically described before calculate hear.

IV. then generated 3-D CAD model using CATIA and import to Simulation software called ANSYS to perform finite element analysis to simulate the heat build-up and the shear stress distribution within the brake.

V. Finally based on the total braking torque generated by brake and temperature distribution, the MRB is investigated and possible improvements that can be made are discussed.

1.5 Scope

Conceptual designs of magnetorheological brake such as material selection and MR fluid selection are considered. Dynamic modal of light rail vehicle is included to calculate braking torque required to stop light rail vehicle. Then 3D a magnetorheological brake modal is generated with CATIA and performs finite element analysis with software called ANSYS to analyze the temperature rise and the shear stress distribution within the brake. Finally the braking torque capacity of brake is investigated theoretically.

1.6 Limitation

In this research, practical design criteria such as material selection and MR fluid selection and the mathematical model which will represent the magnetic circuit and the physical phenomenon of MR fluid brake will be considering to calculate the total braking torque capacity of MRB and

a finite element model to analyze the temperature rise and the shear stress distribution within brake domain. However, detail design of magnetorheological brake, torque to load relationship and test the MRB braking performance using an experimental setup are not considered.

1.7 Significance of the research

Brake-by-wire is a focus topic to improve rail vehicle performance, safety and cost. Brake-by-wire system using an electromechanical brake that replaces the mechanical connection between the brake actuator on each wheel set and the driver's brake valve handle with electrical components. This work is concerned with the development of a new brake-by-wire system for light rail vehicle application, using an electromechanical brake (EMB) that employs magnetorheological (MR) fluid. Benefits are pure electronically controlled brakes systems and as a result, it has the potential to further reduce the braking time (thus, braking distance), reduced wear out of wheels and rail due to more adaptive and economical brake functions, less mechanical and pneumatic components due to replacement of electronic parts and lighter overall weight, at the same time properties and behavior of the brake will be easy to adapt by simply changing electrical inputs instead of adjusting mechanical components. This also allows easier integration of existing and new control features such as anti-lock braking system (ABS), vehicle stability control (VSC), electronic parking brake (EPB), etc.

1.8 Research Outline

The research is organized in eight parts. The first chapter is the introduction part which clearly states the background of the research, statement of problem, and objective, scope and limitation of the study and benefits of the research.

Chapter two discusses literature review of the magnetorheological brake system. Definition, key points, models and analytical approaches will be discussed in this part of the study.

Chapter three shows the dynamic model of a typical passenger light rail vehicle is introduced and the braking torque requirements are calculated for light rail vehicle.

Chapter four discussed the constitutive behavior of the MR fluids and the behavior of MR fluid is modeled using the Bingham plastic model. Then, by using this model, the total braking torque

generated is analytically described in terms of the magnetic field intensity applied and the viscosity of the fluid.

In Chapter five, the design process of a magnetorheological brakes (MRB) such as material selection, MR fluid selection and magnetic circuit design are explained in detail. There are also some additional points are included, braking torque generated which is analytically described in chapter 4 and heat flux applied on brake and convective heat transfer coefficient are calculated. Then a 3-D CAD model of the magnetorheological brake is generated using software, CATIA

In Chapter six, a FEM of the magnetorheological brake (MRB) is created solving the, the shear stress distribution and temperature distribution within the brake, a commercial FEA software package, ANSYIS, is used for this purpose.

In chapter seven, results and discussions which include possible design suggestion will be discussed.

The conclusions of this work are presented in Chapter eight. In addition, possible improvements that can be made are discussed here as part of future works.

CHAPTER TWO

2. REVIEW OF LITERATURE

The introduction of ”x by wire” technologies, electromechanical brakes (EMB) have appeared in the industry. In this configuration, some of the pure mechanical components of the conventional brakes are replaced by electromechanical components. The significance with these new systems is that the vehicle control is quickly evolving away from the limitations of traditional mechanical components. Electric calipers developed by Continental and Delphi are a simple example where the hydraulic actuators are replaced with electromechanical ones [4].

Although the studies on MRFs started around the late 1800s and early 1900s, the first relevant patent was issued to Jacob Rabinow in 1940s [1]. The interest in MR technology rose in the late 1980s and since then, a number of commercial and research devices have appeared: e.g. hydraulic systems, damping systems and seismic devices, clutches, prosthetic devices, haptic devices, cancer treatment equipments and exercise equipments. Also, a study on possible applications of MRF devices was done by Carlson et al. At the same time W. Wislow was working on a competitive technology called electrorheological fluid (ERF). Since the time when both technologies were discovered in the 1940s, there are some similarities between the two different technologies both fluid are linear viscous liquid whose rheological behavior changes. However the main difference is that ER fluid linear behavior changes under the influence of an applied electric field, instead of a magnetic field. Table1 presents a brief comparison between ER and MR fluids [1] [4].

Table 1 ER versus MR fluids [1]

	ER fluids	**MR fluids**
Yield stress	2-5 kPa	50-100 kPa
Operating environment	-25C^{o} to +125 C^{o} Do not tolerate impurities	-40 C^{o} to +150 C^{o} Tolerate impurities
Density	1-2 g/cm^{3}	3-4 g/cm^{3}
Energy density	0.001J/cm^{3}	0.1 J/cm^{3}
Power supply	2-5 kV, 1-10mA	2-25V,1-2A

The idea of using the friction generated by aligned magnetic materials under magnetic field in brakes was first introduced by Eddens. He devised a brake which contains small magnetic particle powder and when magnetic field is applied, the powder aligns in the direction of applied magnetic field and generates a resistance against motion. With the subsequent introduction of MRFs, the dry magnetic particle powder has been replaced by these fluids as the source of friction for braking purposes [4].

The literature presents a number of MR and ER fluid-based brake designs and modeling, optimization and control issues, Karakoc et al. focused on the investigation of practical MR brake design criteria such as material selection, sealing, working surface area, viscous torque generation and MR fluid selection for basic automotive braking system[1]. Furthermore, Tan et al. are studies braking response of inertia/load by using an electro-rheological (ER) brake for ER robotic application in term of ER braking velocity response in order to halt the robot arm rapidly [4]. In 2009, Nam and Ahn is proposed the new structure of MR brake with the waveform boundary of rotary disk that generated more resistance torque compare to the conventional MR brake. Furthermore, the MR brake system had been implemented to other application such as joystick and prosthetic knee [11].

The basic configuration of a MRB proposed by Park et al. for the automotive application is shown in Figure 1. In this configuration, a rotating disk (3) is enclosed by a static casing (5), and the gap (7) between the disk and casing is filled with the MR fluid. A coil winding (6) is embedded on the perimeter of the casing and when electrical current is applied on the coil, due to the generated magnetic fields, the MR fluid in the gap becomes solid-like instantaneously. The shear friction between the rotating disk and the solidified MR fluid provides the required braking torque [4] [1].

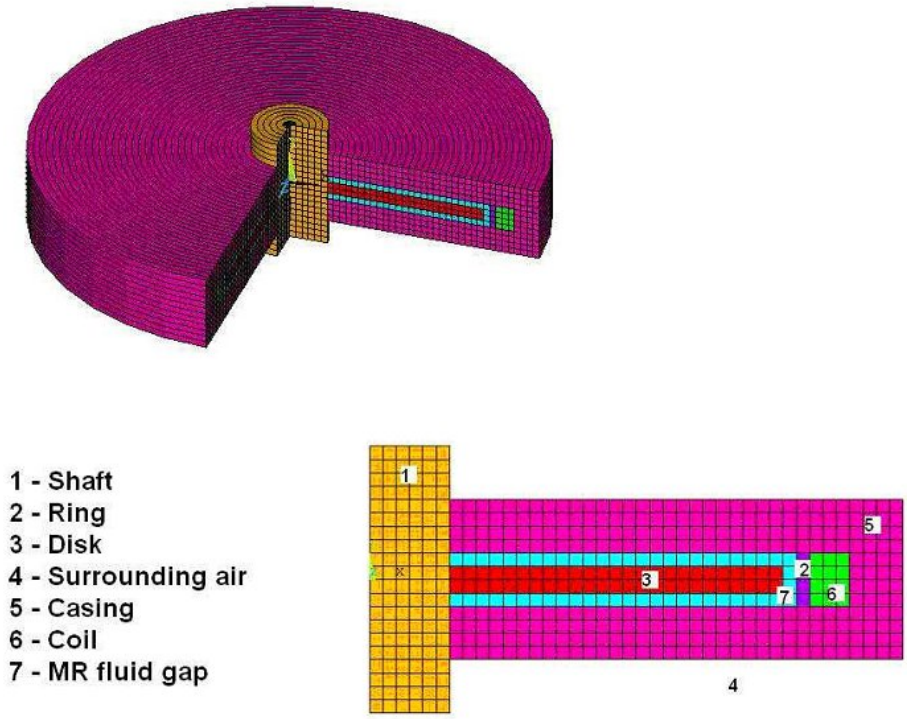

Figure 1 Cross section of an MRB actuator [4]

Nowadays, numerous research activities have been performed in various engineering applications including MR brakes for instance

Edward J Park, Dilian Stoikov, Luis Falcao da Luz and Afzal Suleman [1], the aim of this research is to develop a magnetorheological brake (MRB) system that has performance advantages over the conventional hydraulic brake system. The proposed brake system consists of rotating disks immersed in a MR fluid and enclosed in an electromagnet, which the yield stress of the fluid varies as a function of the magnetic field applied by the electromagnet. The controllable yield stress causes friction on the rotating disk surfaces, thus generating a retarding brake torque. The braking torque can be precisely controlled by changing the current applied to the electromagnet. In this paper, an optimum MRB design with two rotating disks is proposed based on a design optimization procedure using simulated annealing combined with finite element simulations involving magnetostatic, fluid flow and heat transfer analysis. The performance of the MRB in a vehicle was studied using a quarter vehicle model. A sliding mode controller was designed for an optimal wheel slip control, which is a feature of an ABS. The controller maintains the slip ratio at the desired value which assures a maximum braking force

coefficient and provides a minimum stopping distance. The simulation results show the potential of the proposed MRB system to provide fast anti-lock braking. Future work must focus on life-cycle tests to assess the reliability and longevity of the system and to ensure that it can effectively replace the existing hydraulic brake technology. In addition, the proposed MRB can further improved in terms of braking torque, structural weight, and heat dissipation by introducing slots/holes in the rotating disks. The brake weight can be significantly reduced by employing a water-based MR fluid (e.g., Lord Corporation's MRF-241ES), but then the structural design has to be changed to improve heat dissipation capabilities, unless a MR fluid with better temperature properties becomes available.

Edward J Park, Luis Falca˜o da Luz and Afzal Suleman [2], in this research present the development of a new electromechanical brake system using magnetorheological (MR) fluid. The proposed brake system consists of rotating disks immersed in a MR fluid and enclosed in an electromagnet, where the yield stress of the fluid varies as a function of the magnetic field applied by the electromagnet. The controllable yield stress causes friction on the rotating disk surfaces, thus generating a retarding torque. The braking torque can be precisely controlled by simply changing the current applied to the electromagnet. Key issues involved in the initial design of the automotive MR brake are presented such as the MR fluid selection, magnetic circuit design, torque requirements, weight constraints, dimensions and temperature. A multidisciplinary finite element analysis is performed involving magnetostatics, fluid flow, and heat transfer analysis to study the behavior of the system, and to serve as basis for a multidisciplinary design optimization methods were used and compared to obtain ideal dimensions for the brake, so that the sufficient braking torque could be provided by a light-weight MRB. The results obtained with the three methods were compared both in terms of their final output values and the computation time required. As expected, it was found that simulated annealing yields the best result, albeit at a computational cost. The proposed MRB is naturally a pure electronically controlled brake system that uses the use of ‘‘bytes and amperes instead of bars and compressed brake fluid.’’ This allows easy implementation of advanced braking control features with a smaller number of components, simplified wiring, improved braking response and generally optimized layout. In this work, it was shown that the proposed MRB can meet the design targets in terms of braking torque, temperature and weight. Ensure that it can effectively replace the existing hydraulic brake technology. In addition, the proposed MRB can further

improved in terms of braking torque, structural weight, and heat dissipation by introducing slots/holes in the rotating disks or using a water-based MR fluid with better temperature properties.

Kerem Karakoc, Edward J Park and Afzal Suleman [3], in this research design considerations for building an automotive magnetorheological (MR) brake are discussed. The proposed brake consists of multiple rotating disks immersed in a MR fluid and an enclosed electromagnet. When current is applied to the electromagnet, the MR fluid solidifies as its yield stress varies as a function of the magnetic field applied. This controllable yield stress produces shear friction on the rotating disks, generating the braking torque. Practical a magnetorheological brake (MRB) design has been introduced as a viable alternative to the current conventional hydraulic brake (CHB) device. Since the MRB is an electromechanical device, it has several advantages over the CHB, such as reduced actuation delay, ease of software control implementation and lower system weight. The design process was started with an analytical model of the MRB. Then, the MRB device was designed with a focus on magnetic circuit optimization and material selection. A two-dimensional finite element model of the MRB was created to simulate the steady-state magnetic flux flow within the MRB domain using COMSOL electromagnetic module and solve for the magnetic field intensity distribution. In addition to the detailed electromagnetic analysis, a simple heat transfer analysis was carried out to monitor the heat build-up within the brake. The FEM was then used to optimize the magnetic circuit design in order to maximize the braking torque and minimize the weight of the MRB. The optimization problem was solved using a hybrid optimization procedure that included simulated annealing and sequential quadratic programming algorithm. A 3-D CAD model of the optimum MRB design was generated and a MRB prototype of the optimum design was manufactured. The MRB braking performance was tested using an experimental apparatus that consisted of a torque sensor and a servo motor show a good correlation with the finite element simulation predictions. However, the braking torque generated is still far less than that of a conventional hydraulic brake, which indicates that a radical change in the basic brake configuration is required to build a feasible automotive MR brake.

M. Kciuk and R Turczyn [6], this paper presents basic properties of the magnetorheological fluids (MR) and their development in recent years. A variety of still growing practical

applications in mechanical devices are presented. The theoretical research results of the properties and applications obtained in the past decades and progressed in recent years are reviewed. It is very clearly and well understood from the presented paper that replacement of the traditional devices with active, smart system better adapted to the environment stimulus are necessary. Many of them will include MR fluids as active component.MR fluids with excellent properties can be applied in various fields of civil engineering, safety engineering, transportation and life science. They offer an outstanding capability of active control of mechanical properties. A very useful material for the engineers engaged in the design of brakes, dampers, clutches and shock absorbers systems. This article describes an up-to-date MR materials development and their application in civil engineering. The advantage of the smart systems over nowadays solutions becomes the direction of the researches and designing of 21st century devices.

Mukund A.Patil and Ashutosh S.Zare [8], in this research, the design method of the cylindrical MR fluid brake is investigated theoretically .a magnetorheological (MR) fluid brake is a device to transmit torque by the shear force of an MR fluid. An MR rotary brake has the property that its braking torque changes quickly in response to an external magnetic field strength. The mechanical part is modeled using Bingham's equation, an approach to modeling the magnetic circuit is proposed in this work. The equation of the torque transmitted by the MR fluid within the brake is derived to provide the theoretical foundation in the cylindrical design of the brake. Based on this equation, after mathematical manipulation, the engineering design calculations of the volume, thickness and width of the annular MR fluid within the brake are derived. When the required mechanical power level, the rotational speed of the rotor, and the desired control torque ratio are specified, the parameters of the thickness and width of the fluid in the brake can be calculated from the equations obtained.

Luo Yiping, Xu Biao, Ren Hongjuan and Chen Fuzhi [10], Based on this research of the new material magnetorheological fluid dynamometer is designed. Under the premise of certain structure size and material, there is a one-to-one correspondence between MRF dynamometer loading current and load torque provided with the machine electricity and the theoretical calculation. This paper gives the design method and specific geometric parameters of magnetorheological fluid dynamometer. The process of magnetorheological fluid dynamometer

theory design is obtained by taking a specific model motor as an example, which provides a theoretical basis for the application of MRF in the field of dynamometer. The following conclusions are drawn.

1. put forward a new theoretical dynamometer design method, the calculation process of torque and reluctance during the design of magnetorheological fluid dynamometer and a determination method of current, turns, diameter and other parameters.
2. Taking some motor as example into practice proves its feasibility of this method enlarges dynamometer range and provides a theoretical basis for the design of magnetorheological fluid dynamometer.
3. Magnetorheological fluid dynamometer design process still have some problems, such as sealing, cooling and control problems. If these problems are solved, the design of the dynamometer will be more perfect.

Ahmad Zaifazlin Zainordin, Mohd Azman Abdullah, and Khisbullah Hudha [11], in this research present experimental evaluation on braking responses of magnetorheological brake (MR Brake) at various current and load. The MR brake consists of a rotating disk that immersed with magnetorheological fluid (MR fluid) where the fluid behavior is changing under influence of magnetic fields. The experiments are performed using MR brake test rig to obtain three output responses namely the angular velocity response, torque response and load displacement response. The MR brake generates maximum torque at high current and causes fast decrement of shaft angular velocity. The effectiveness MR brake torque happens at minimum load with low stopping time. Generally, the applied current to the MR brake will decrease all the inertia to stationary. When applied constant current, the MR brake generated net torque at constant torque with respect with applied current. However, when increased the load will caused the MR brake takes longer settling time and the load displacement response becomes longer to constant steady-state displacement. Furthermore, the heavier load will reduce the effectiveness of MR brake torque. The effective ranges of MR brake torque are 50N until 100 N.

Mr. Vinayak D. Dabade, Prof. Y. R. Patil, Prof.M.V. Kharade and Prof. P.R. Patil [18], in this research the geometric design method of a cylindrical MR fluid brake is presented theoretically.

Based on a commercially available magneto rheological fluid, a new automotive brake system was proposed. The model of the proposed MRB was presented, an optimum MRB design with two rotating disk was proposed. The proposed MRB is naturally a pure electronically controlled brake system that uses the use of bytes and amperes instead of bars and compressed brake fluid. This allows easy implementation of advanced braking control features with a smaller number of components, simplified wiring, improved braking response and generally optimized layout. In this paper, also presented theoretically magneto rheological dampers of various applications have been and continue to be developed. The MR damper contains the fluid and an electric coil, which generates a magnetic field that controls fluid viscosity at any given moment. The overall MR suspension system also consists of a controller that manages the strength of the magnetic field applied to the fluid. Vibration in today's increasingly high-speed vehicles including automobiles severely affects their ride comfort and safety. To improve the ride comfort, effective vibration control of suspension systems implement car suspension system with a MR fluid damper. It is very clearly and well understood from the presented paper that replacement of the traditional devices with smart system. Properties of the magnetorheological fluids (MR) and their development in recent years, many of them will include MR fluids as active component. A very useful material for the engineers engaged in the design of brakes, dampers, clutches and shock absorbers systems.

Giuseppe Marannano, Gabriele Virzi Mariotti and Cedomir Duboka [19], in this research presents the optimization process of magnetorheological brake in order to define its configuration and to reach the requested vehicle braking torque, FEM analysis previously carried out, concerning structural sizing of such a brake, showed that both braking torque and brake mass did not satisfy the requirements. Due to the necessity of limitation on the suspended mass of a motor vehicle, the optimization of the form of MR brake stator has been executed, including determination of its contribution to the total mass of the brake. In order to verify its ability to satisfy both braking torque and mass requirements for a vehicle brake. Thus a percentage reduction of approximately 40% was obtained. A thermal finite element analysis is carried out in order to estimate the brake temperature which results from the transformation into heat of a vehicle kinetic energy during brake application, in particular a fade braking test composed of snub braking, i.e. repeated cycles of acceleration and consecutive braking applications is performed. The obtained results of thermal analysis highlight a maximum temperature within the

limit operating value of the fluid. However, cooling of the brake to remove the heat over the active surfaces is necessary in the hypothesis of employment of the brake in more severe conditions of application. This could be put into effect to achieve fins in the stator, that increase the surface of thermal exchange with the environment, or a cooling of "active" type, taking advantage of the system already presented on the vehicles. Advantages derived from the use of MR brake in place of a conventional brake (disc or drum) for motor vehicle are significant. In the first instance, MR brake provides reduced response time compared to hydraulically and/or air operated brake and it takes some time to raise the line pressure of the fluid to initiate braking. The greater response time brings reduction of the space, making, therefore, braking results more effective. The substitution of the conventional hydraulic braking system with an electrically operated system offers advantages in terms of simplicity of configuration and better solutions of housing.

Mohammadhossein Hajiyan, Shohel Mahmud, and Hussein A. Abdullah [20], In this research presents a novel design of multi-disks magnetorheological braking system (MR brake) for automotive application. Magnetic saturation in both electromagnetic core and MR fluid is considered in this paper. The electromagnetic analysis of the proposed conguration is carried out using finite element based COMSOL multiphysics software (AC/DC module). The system geometry, created using AutoCAD software, is discretized using a finite number of triangular elements with a higher concentration of elements near the internal boundaries. Post processing option of COMSOL multiphysics software is utilized to calculate the magnetic fled distribution and magnetic flux density inside the MR fluid and electromagnetic core. A one dimensional analytical model is developed to calculate the braking torque of the proposed system. The performance of the proposed design shows improvement over the designs available in the existing literature considering the same dimensional restrictions.

Unlike previous works, in this work, a new MRB is design and develop for light rail vehicle with a focus on magnetic circuit design and material selection.

CHAPTER THREE

3. DYNAMIC MODEL OF A LIGHT RAIL VEHICLE

In order to determine braking torque, the technical data of light rail vehicle and its dynamic parameter are required. These parameters were taken from Addis Ababa LRT project study report and are listed in table 2

Table 2 Tramcar parameters were taken from Addis Ababa LRT project study report

parameter	value
Wheel Base for power bogie for driven bogie	1900mm 1600mm
Wheel Diameter Motor Wheel Driven Wheel	660mm 600mm
Tramcar Width	2650mm
Tramcar Height	3700mm
Tramcar Length	28400 mm
The Highest Speed	80Km/h
Weight of Tramcar	43t
Average Acceleration for Start -Up	1m/s^2 （0-40Km/h）
Average Deceleration for Braking: from	80Km/h to stop
Ratio of Acceleration and Deceleration:	0. 75m/s^2
The Average Deceleration of Normal Braking with Rated Load including (control response time)	≥1.0m/s^2
The Average Deceleration of Emergent Braking with Rated Load （including control response time）	≥1.5m/s^2

3.1 Kinematics equation of braking

The railway tramcar running with initial velocity (v_o) is supposed to stand still with constant deceleration (a). Its linear translational velocity as function of time (t) is given by:

$$v(t) = v_o - at \quad \text{.....3.1}$$

I. The angular velocity (ω) of the wheel set can be determined using

$$\omega = \frac{v_o}{r_w} \quad \text{.....3.2}$$

Where

v_o = velocity of the tramcar

r_w = the radius of wheel

From tble 2 the highest speed of light rail vehicle and wheel diameter is taken 80Km/h (22.2m/s), 660mm (r_w=0.33m)

$$\omega = \frac{22.2}{0.33}$$

$$\omega = 68 rad/s$$

II. The total braking distance can also be calculated by the formula [9]:

$$v_f^{\,2} = v_o^{\,2} + 2as \quad \text{..... 3.3}$$

Where

v_f is final velocity

v_o is initial velocity

a is deceleration during braking

s is brake distance

In case where the deceleration is full stop v_f is zero and s is the stopping distance then [9]

$$S_b = \frac{v_o^{\,2}}{2a} \quad \text{.....3.4}$$

From table 2 average deceleration for braking from 80km/h (22.2m/s) to stop and the average deceleration 1.5m/s^2

$$S_b = \frac{22.2^2}{2 \times 1.5}$$

$$S_b = 164.3m$$

III. Time to stop during braking

$$V_f = V_o - at \quad \text{.....3.5}$$

$$V_f = 0\ , \qquad t_b = \frac{V_o}{a}$$

$$t_b = \frac{22\ .2}{1\ .5} = 14.8\text{s}$$

IV. Angular deceleration α of wheel

$$\alpha = \frac{\omega}{t} \quad \text{.....3.6}$$

Where, ω is angular velocity of wheel and *t* is time

$$\alpha = \frac{68}{14.8}$$

$$\alpha = 4.6\, rad/s^2$$

3.2 Loading Capacity/Carrying Capacity of train

Table 3 Loading capacity/carrying capacity of train

Status	Seat	Standing Capacity	Total
Rated capacity (AW3)(Standing capacity:8persons/m^2)	64	190	254

[Source: Addis Ababa (E-W and N-S) rout light rail transit project from ERC, September 2009]

3.2.1 Train Weight

Table 4 Train Weight

Status	Appr. Weight of train body (t)	Passenger Weight (t)	Total (t)
Rated capacity (AW3)(Standing capacity:8persons/m^2)	48.76	15.24	64

Note: passenger weight 60kg/person

[Source: Addis Ababa (E-W and N-S) rout light rail transit project from ERC, September 2009]

3.3 Kinetics of braking

In this work, the brakes are installed on each wheel there for the braking of a light rail vehicle is considered using the 1/8 of vehicle model .This model is needed to calculate the required braking torque that a brake should provide. The basic assumption of this model is that the weight of the vehicle is divided equally between eight wheels. In figure 2, a free body diagram of a wheel rotating clockwise is shown. During braking, a torque is applied by the brake, T_b, and F_r, F_f, F_n and F_L are the rolling resistance force, the friction force, normal force and the transfer of weight caused by braking of the vehicle. Let's denote I as the total mass moment of inertia and α is the angular acceleration of the vehicle. The radius of the wheel is R_w and x is the distance traveled by the vehicle.

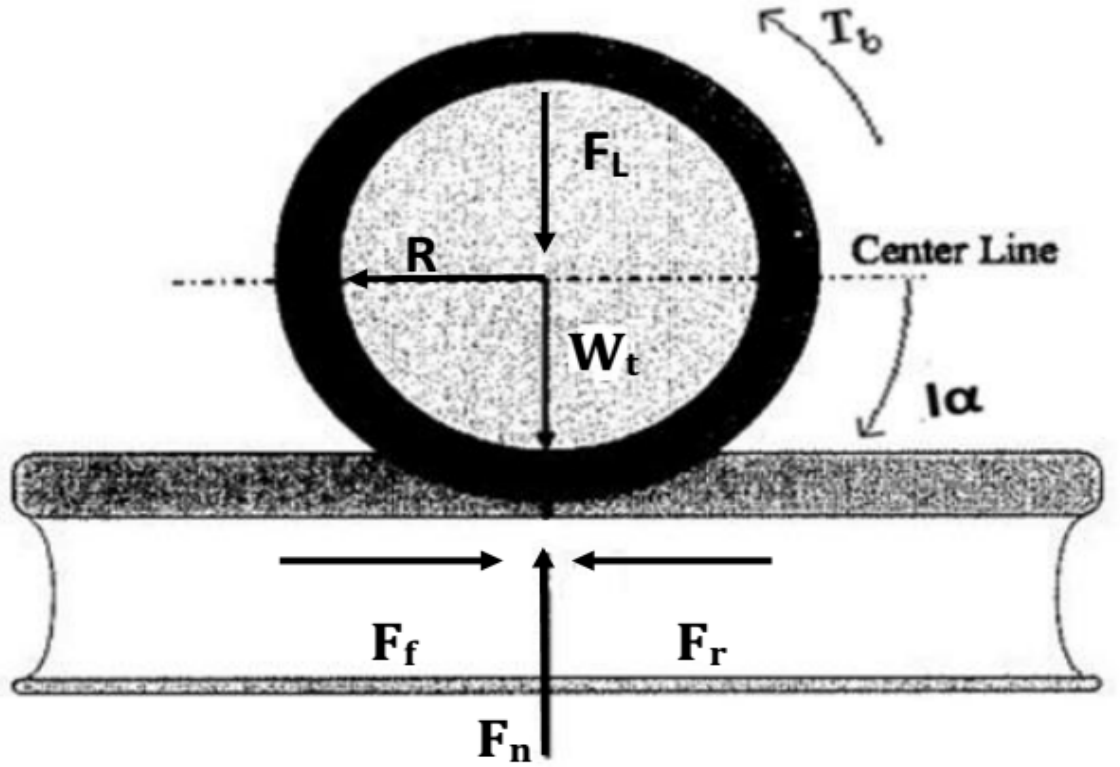

Figure 2 Free body diagram of a wheel [21]

I. The equivalent weight that the wheel carries can be calculated as [4]

$$W_t = \frac{1}{8} m_v g + m_w g \quad \text{..... 3.7}$$

Where

m_v is total mass of the vehicle and passenger

m_w is the mass of the wheel.

According to the UIC, S1002 railway standard the mass of the wheel are selected to be 230Kg, from table 4 weight of tramcar 64tone

$$W_t = \left(\frac{1}{8} \times 64000 + 230 \right) \times 9.81$$

$$W_t = 80.74 \times 10^3 N$$

II. The rolling resistance force against the motion of the wheel is defined as[21]

$$F_r = 0.75 W_{WS} + 9.02 + 0.0305 W_{WS} V_{WS} \quad \text{..... 3.8}$$

Where

W_{WS} is weight on each wheel set in tones

V_{WS} is velocity of the wheel set

from table 2, V_o = 80Km/h or 22.2m/s and from above calculation weight on each wheel set in tones is $8.23 tones$ then rolling resistance force against the motion of the wheel become

$$F_r = 0.75 \times 8.23 + 9.02 + 0.0305 \times 8.23 \times 22.2$$

F_r=20.77N

III. the normal force between the wheel and the rail surface is determined as

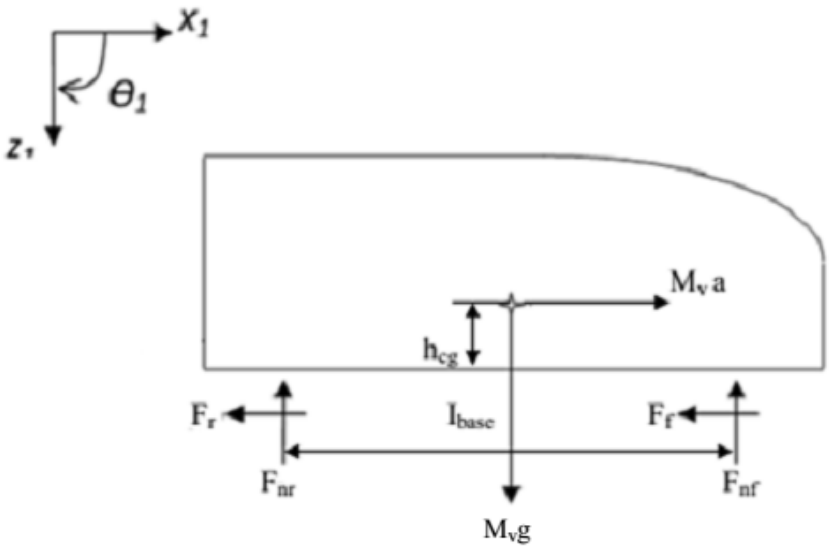

Figure 3 Free body diagram of light rail vehicle body

The normal force between each wheel and the rail surface is given by

$$F_n = W_t + \frac{m_v h_{cg}}{\mathrm{I}_{base} \times 4} a \quad \text{.....3.9}$$

Where

l_{base} is the wheel base and

h_{cg} is the height of the center of gravity

$\mathrm{W_t}$ is the equivalent weight that the wheel carries

a is deceleration

m_v is total mass of the vehicle and passenger

From table 2 the average deceleration of emergent braking with rated load 1.5m/s^2 and wheel base 1900mm and from table 4 total mass of the vehicle and passenger is 64000Kg

$$F_n = 80.74 \times 10^3 + \frac{64000 \times 1.85}{1.9 \times 4} \times 1.5$$

$$F_n = 104.1 \times 10^3 N$$

IV. The friction force acting on the wheel is defined in terms of the normal force and the friction coefficient between the tire and the surface, i.e.

$$F_f = \mu_f F_n \quad \text{.....3.10}$$

Where

μ_f is the friction coefficient b/n wheel and rail

F_n is the normal force

Assume dry and smooth rail condition the friction coefficient b/n wheel and rail at 80Km/h under good rail condition is 0.1425. The friction force acting on the wheel is calculated as follows

$$F_f = 0.1425 \times 104.1 \times 10^3$$

$$F_f = 15 \times 10^3 N$$

V. The total mass moment of inertia can be defined by[21]:

Total moment of inertia of wheel and traction motor become $125\,Kgm^2$

VI. Finally, the equations of motion for the wheel can be written as [4] [1]

$$m_t \ddot{x} = -F_f = -W_t \mu_f - \mu_f \frac{m_v h_{cg}}{\mathrm{I}_{base} \times 4} a \quad \text{.....3.11}$$

$$\mathrm{I}\alpha = -T_b + R_w F_f - R_w F_r = -T_b + \mu_f R_w F_n - R_w F_r \quad \text{.....3.12}$$

Eq 3.12 is the force equilibrium equation in the direction of motion and Eq. (3.13) is the moment equilibrium equation around the wheel axis. Then, the required braking torque, T_b, can be found by solving these two equations.

Required braking torque to stop light rail vehicle can be calculate by rearranging Eq 3.13 as follow

$$T_b = R_w F_f - R_w F_r - I\alpha \quad \text{.....3.13}$$

Where

R_w is the radius of the wheel

F_f is the friction force acting on the wheel

F_r is the rolling resistance force against the motion of the wheel

I is total mass moment of inertia

α is the angular acceleration of the vehicle

From table 2, R_w is 0.33m, from kinematics equation of braking (section 3.1) we know α is $4.6 rad/s^2$ and from kinetics of braking (section 3.3) we know F_r is 20.77N, I is $125 Kgm^2$ and F_f is $15 \times 10^3 N$

$$T_b = 0.33 \times 15 \times 10^3 - 0.33 \times 20.77 - 125 \times 4.6$$

$$T_b = 4368.15 Nm$$

Therefore $4368.15 Nm$ the braking torque required for vehicles to stop and the above study was carried out in order to determine the braking torque that a comparable MRB should generate and gives us an idea about how much braking torque must be generated by an MRB to stop light rail vehicle.

CHAPTER FOUR

4 MODELING OF MR BRAKE

4.1 Properties of MR Fluids

A magnetorheological fluid (MR fluid) is a type of smart fluid in a carrier fluid, usually a type of oil. Normally, MR fluids are free flowing liquids having a consistency similar to that of motor oil (Fig. 4). In the absence of an applied field, MR fluids are reasonably well approximated as Newtonian liquids.

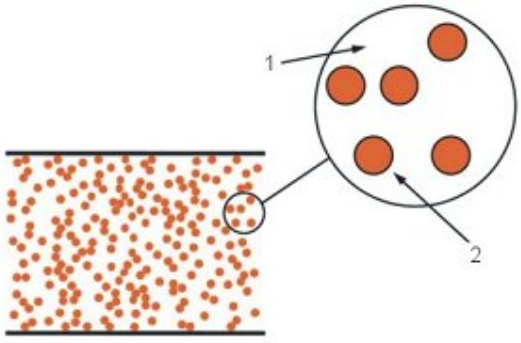

Figure 4 MR Fluid model without outer magnetic field [18], (1) carrier liquid, (2) suspended magnetizabel particle

However, in the presence of an applied magnetic field, the iron particles acquire a dipole moment aligned with the external field which causes particles to form linear chains aligned to the magnetic field, as shown in (fig. 5). This phenomenon can solidify the suspended iron particles and restrict the fluid movement. Consequently, yield strength is developed within the fluid. The degree of change is related to the magnitude of the applied magnetic field, and can occur in a few milliseconds [6].

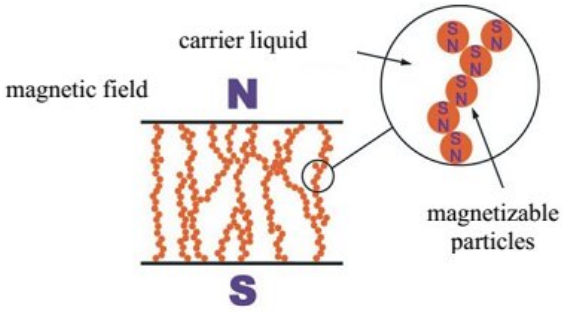

Figure 5 MR Fluid model in outer magnetic field [18]

4.2 Mathematical analysis of magnetorheological brake modeling

For most engineering applications in order to model an MRB, the behavior of the MR fluid under magnetic field application has to be modeled. The idealized characteristics of the MR fluid can be described effectively by using the Bingham-Plastic model [4]. A Bingham plastic is a non-Newtonian fluid whose yield stress must be exceeded before flow can begin. Thereafter, the rate-of-shear vs. Shear stress curve is linear [2].

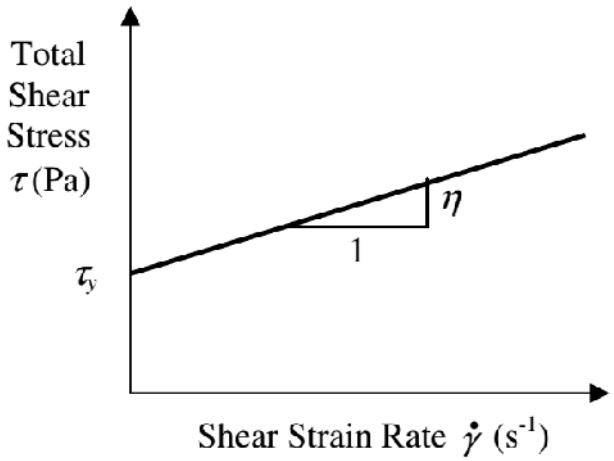

Figure 6 Bingham's plastic model [2]

In the absence of an applied magnetic field, the particles in MR fluid disperse randomly in the carrier fluid. MR fluid flows freely through the working gap, where the shear stress of MR fluids can be described as [1],

$$\tau = \eta\gamma \quad \text{.....4.1}$$

Where

η is the viscosity of the MR fluid with no applied magnetic field, and

γ is the shear rate.

When the magnetic field is applied, the behavior of the controllable fluid is often represented as a Bingham fluid having variable yield strength. In this model, the total shear stress of MR fluids can be described as

$$\tau = \tau_{H} + \eta\gamma \quad \text{.....4.2}$$

τ_H is the yield stress developed in response to the applied magnetic field

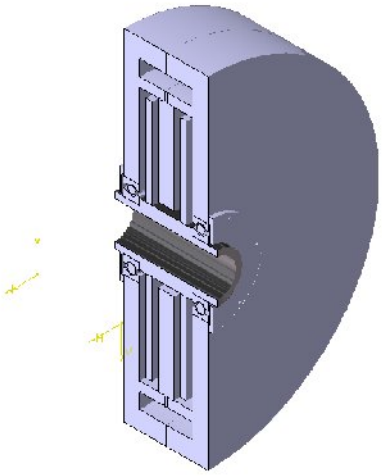

Figure 7 Magnetorheological Brake modal

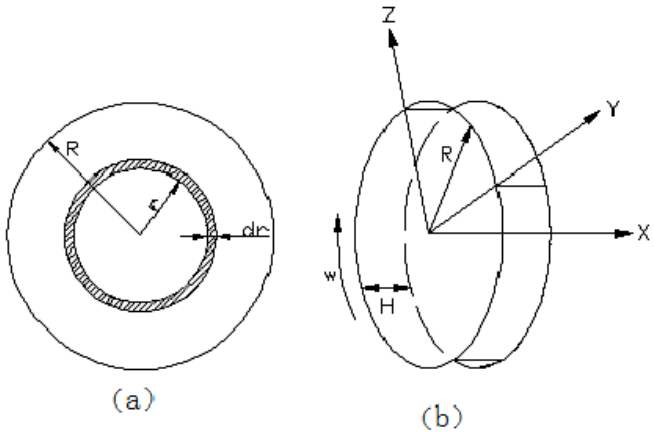

Figure 8 Magnetorheological fluids torque analytical diagram

Integrate Eq 4.2 at the given geometrical configuration shown in fig. 8, the retarding or braking torque which is caused by the friction on the interfaces between the MR fluid and the solid surfaces within the MR brake can be written as

$$T_b = 2\pi N \int_{R_1}^{R_2} \tau r^2 dr = 2\pi N \int_{R_1}^{R_2} \left(\eta\gamma + \tau_H\right) r^2 dr \quad \text{..... 4.3}$$

Where

N is the number of surfaces of the brake disk(s) in contact with the MR fluid

R_2 is the outer radii of the brake disk and

R_1 is inner radii of the brake disk

The shear deformation rate can be calculated by

$$\gamma = \frac{r\omega}{h} \quad \text{..... 4.4}$$

Where

ω is the angular velocity of the rotating disk,

h is the thickness of the MR fluid gap

The yield stress developed in response to the applied magnetic field can be calculated

$$\tau_{H} = \mathrm{KH}^{\beta} \quad \text{.....4.5}$$

K and β are constant parameters that approximate the relationship between the magnetic field intensity and the yield stress for the MR fluid.

Then, Eq. (4.3) can be rewritten

$$T_b = 2\pi N \int_{R_1}^{R_2} \left(\eta \frac{r\omega}{h} + \mathrm{KH}^{\beta} \right) r^2 dr \quad \text{.....4.7}$$

Then, Eq.4.7 can be divided into the following two parts

a) Torque generated due to the viscosity of the fluid.

$$T_{\eta} = 2\pi N \int_{R_1}^{R_2} \left(\eta \frac{r\omega}{h} \right) r^2 dr \quad \text{.....4.8}$$

Performing the integration in Eq. (4.8) and

$$T_{\eta} = \frac{\pi}{2h} N \eta \omega \left(R_2^{\,4} - R_1^{\,4} \right) \quad \text{.....4.9}$$

b) Torque generated due to the applied magnetic field

$$T_H = 2\pi N \int_{R_1}^{R_2} \left(\mathrm{KH}^{\beta} \right) \times r^2 dr \quad \text{.....4.10}$$

The braking torque induced by the magnetic field can be calculated with assuming that the shear stress is constant over the active MR area [12] Performing the integration in Eq.(4.10)

$$T_H = \frac{2\pi}{3} N \mathrm{K} H^{\beta} \left(R_2^{\,3} - R_1^{\,3} \right) \quad \text{.....4.11}$$

Finally, the total braking torque

$$T_b = T_H + T_{\eta} \quad \text{.....4.12}$$

CHAPTER FIVE

5 DESIGN OF MR BRAKE

5.1 Conceptual Design

In this section, the proposed MR brake was designed considering the design parameters addressed in the previous section. In addition, some of the key practical design considerations were also included during the design process for the brake are listed, which will be discussed in detail in this section. Note that fig. 7 show the cross-section of the MRB which was designed according to the listed design criteria. This is the basic configuration that will be considered for finite element analysis.

- Material selection
- MR fluid selection
- Magnetic circuit design

5.2 Material selection

The material selection is another critical part of the MRB design process. Materials used in the MRB have crucial influence on the magnetic circuit as well as the mechanical and thermal characteristics. Here, the material selection issue is discussed in terms of the magnetic properties and mechanical and thermal properties.

5.2.1 Magnetic properties

The main parameter that defines a material's magnetic characteristics is its permeability (μ). It is the ability of the material to transfer magnetic flux over itself. In the literature, relative permeability (μ_r), which is the ratio between the material's permeability and vacuum's permeability (i.e. $\mu_0 = 4\pi 10^{-7}$H/m), is commonly used [3][4].

Materials are classified in three groups according to their permeability values:

i) ferromagnetic materials,

Materials that are strongly attracted by the applied magnetic field are ferromagnetic materials. They have permeability of higher than 1.

Table 5 Comparisons of the properties of ferromagnetic material B_m are values of the magnetic flux density at saturation μ_r are relative permeability values [12]

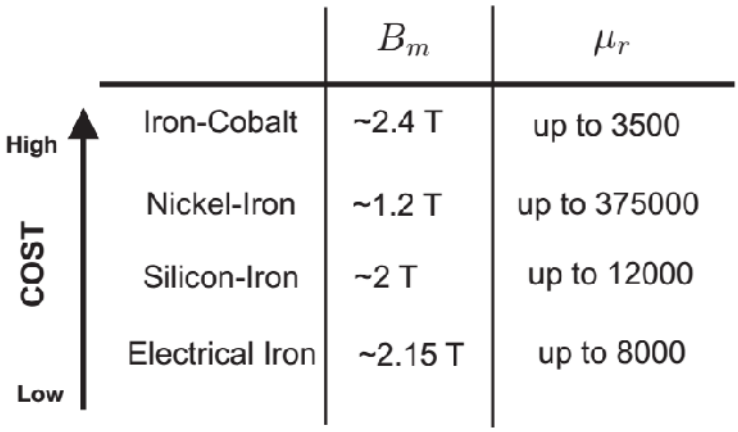

ii) Paramagnetic materials

The materials that are attracted weakly by the applied magnetic field are paramagnetic materials and their permeability is close to 1, most of the paramagnetic materials have permeability between 1 and 1.001

iii) Diamagnetic materials.

The last group of materials is the diamagnetic materials, which are repelled by the applied magnetic field. These materials have a tendency to move toward the weaker field. They have permeability smaller than 1[3][4].

As ferromagnetic materials, there is a wide range of alloy options that are undesirably costly for brake application. Therefore, a more cost-effective material with required permeability should be selected. By considering the cost, permeability and availability, low carbon steel, AISI 1018 was selected as the magnetic material for the magnetic circuit (i.e. the shear disk)

Table 6 Properties of STEEL1018 [4]

Property	STEEL 1018
Composition	C-0.15/0.2%,Mn-0.6/0.9%, P and S
Tensile Strength(MPa)	634
Yield Strength(MPa)	386
Hardness Rockwell B	197
Density(Kg/m^3)	7700-8030
Modulus of Elasticity(GPa)	190-210
Thermal Conductivity (W/m-K)	51.9
Specific Heat(J/Kg-K)	486

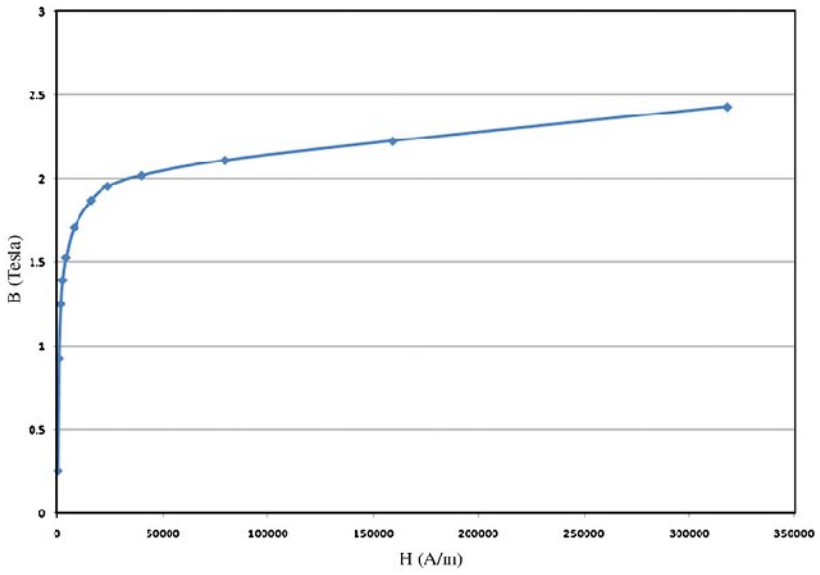

Figure 9 B-Hcurve of steel 1018 for initial loading [3]

5.2.2 Structural and thermal characteristics

In terms of mechanical property, there are two critical parts the shaft and the shear disk. The shaft carries the brake and transfers the torque generated by the MRB and the shear disk where the braking torque is generated. The shaft should be non-ferromagnetic in order to keep the flux far away from the seals that enclose the MR fluid[3][4], due to its high yield stress and availability 304 stainless steel is a suitable material for the shaft.

Table 7 Properties of SS304 [4]

Property	SS304
Composition	Cr-18/20%,Ni-8/10.5%,Mn-2%,Si-1%, C-0.08%,P and S
Tensile Strength(MPa)	515
Yield Strength(MPa)	205
Hardness Rockwell B	88
Density(Kg/m^3)	8000
Modulus of Elasticity(GPa)	193
Thermal Conductivity (W/m-K)	16.2
Specific Heat(J/Kg-K)	500

5.3 MR fluid selection

There are a number of commercial MR fluids available from Lord Corporation [3]. No-field viscosity of the MR fluid, operating temperature range and shear stress gradient are some of the key properties that have to be considered when making a selection. According to No-field viscosity of the MR fluid and shear stress gradient MRF-132DG is the best candidate for the braking application. There for MRF-132DG is suitable for this research.

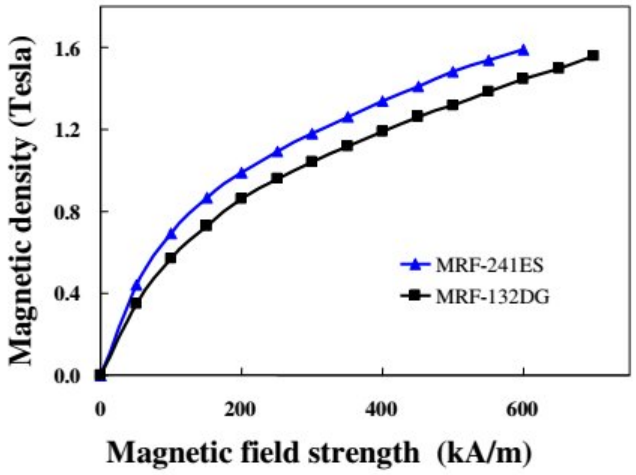

Figure 10 B-H curves for MRF-241ES and MRF-132DG [13]

Table 8 properties of MRF-132DG [4] [3]

Property	Value/limits
Base Fluid	Hydrocarbon
Operating Temperature	-40 to 130℃
Density	3.09 g/cc
Weight Percent Solid	81.64 %
Coef. of Thermal Expansion (Unit Volume per ℃) 0 to 50℃ 50 to 100℃ 100 to 150℃	 5.5e-4 6.6e-4 6.7e-4
Specific Heat at 25℃	0.80 j/g℃
Thermal Conductivity at 25℃	0.25-1.06 w/m℃
Viscosity ,η(no magnetic field applied) slop between 500 and 800 s^{-1}	0.09 ± 0.02 Pa s
Flash Point	-150℃
K	0.269 Pa-m/A
β	1

5.4 Magnetic circuit design

The main goal of the magnetic circuit analysis performed in this work is to direct the maximum amount of the magnetic flux generated by the electromagnet onto the MR fluid located in the gap. This will allow the maximum braking torque to be generated.

5.4.1. Saturation flux density of selected materials

a) Low carbon steel, AISI 1018

From section 5.2 a material used for the magnetic structure(including left and right shell, outer race and the shear disk) around coil is low carbon steel, AISI 1018 which relative permeability that can increase from the initial several hundreds to thousands under different magnetic induction intensity, but we ignore the change and choose relative permeability $\mu_{rA} = 800$ [10], from figure 11 Saturation flux density is B_A=2.4T

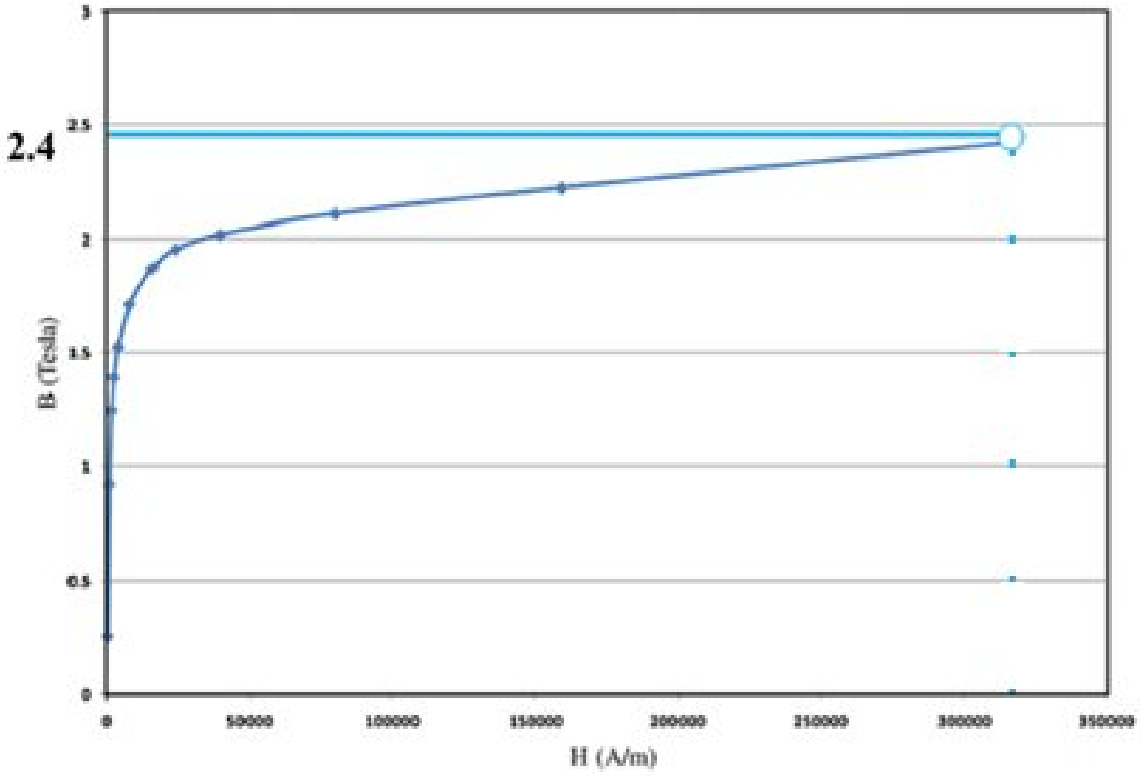

Figure 11 Saturation point of low carbon steel, AISI 1018[3]

b) Magnetorheological fluid

From section 5.3 magnetorheological fluid selected for this work is MRF-132DG. To make full use of magnetorheological fluid, it should saturate first and from (figure 12) B-H curve a saturation flux density of MRF-132DG B_H is 1.6T and whose relative permeability can increase under different magnetic induction intensity, but we ignore the change and choose relative permeability $\mu_{rMRF} = 8$ [10].

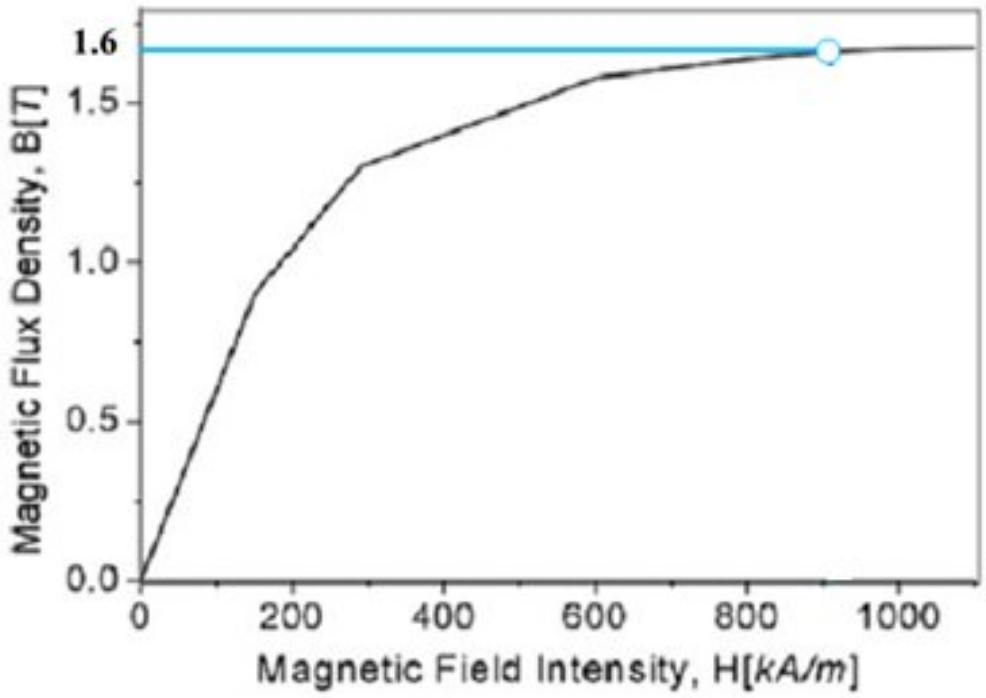

Figure 12 Saturation points of MRF-132DG [14]

5.4.2. Mathematical analyses of magnetic circuit

As shown in figure13 the magnetic circuit in the MRB consists of the coil winding in the electromagnet, which is the magnetic flux generating ”source” (i.e.by generating magnetomotive force or mmf), and the flux carrying path. The path provides resistance over the flux flow, and such resistance is called reluctance ($\Re$) [3] [4]. Thus, in Figure 14, the total reluctance of the magnetic circuit is the sum of the reluctances of the core and the gap, which consists of the MR fluid and the shear disk then, the flux generated (ϕ) in a member of the magnetic circuit in figure 13 can be defined as:

$$\phi = \frac{ni}{\Re} = \frac{mmf}{\Re} \quad \text{.....5.1}$$

Where

ni is magnetomotive force or mmf

$\Re$ is reluctance

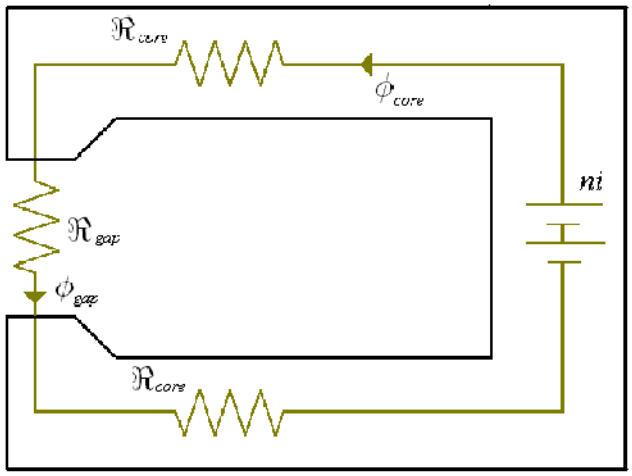

Figure13 Magnetic circuit represent of MRB [4] [3]

According to [3][4][8][10] reluctance ($\Re$) can be calculated

$$\Re = \frac{l}{\mu A} \quad \text{.....5.2}$$

Where

$$\mu = \mu_o \mu_r \quad \text{.....5.3}$$

μ_r is relative permeability of material

μ_o is vacuum's permeability (i.e. $\mu_0 = 4\pi 10^{-7}$H/m)

In Eq. (5.1), n is the number of turns in the coil winding and i is the current applied; recall that in order to increase the braking torque, the flux flow over the MR fluid needs to be maximized. This implies that the reluctance of each member in the flux path of the flux flow has to be minimized according to Eq. (5.1), which in turn implies that length (l) can be decreased or/and permeability of material (μ) and cross-sectional area (A) can be increased according to Eq. (5.2).

Thus, in figure 14 loop is series arrangement there for the total reluctance of the magnetic circuit is the sum of the reluctances of the core and the gap, which consists of the MR fluid and the shear disk.

As shown in figure14, when magnetic circuit passes left of shear discs 3, and right of shear disc 8 because they are symmetrical, substituted formula (5.2) gives

$$\Re_3 = \frac{L_2}{\pi\left(R_2^{\ 2} - R_1^{\ 2}\right)\mu_3} \quad \text{.....5.4}$$

$$\Re_3 = \Re_8$$

As shown in figure14, when magnetic circuit passes outer race 1 and magnetorheological fluid 4, substituted formula (5.2) and we get:

$$\Re_1 = \frac{L - L_1}{\pi\left(R_4^{\ 2} - R_3^{\ 2}\right)\mu_1} \quad \text{.....5.5}$$

$$\Re_4 = \frac{h}{\pi\left(R_2^{\ 2} - R_1^{\ 2}\right)\mu_4} \times 4 \quad \text{.....5.6}$$

As shown in figure14, when magnetic circuit passes left and right shell, because they are symmetrical, substituted formula (5.2) and we get

$$\Re_2 = \frac{\left(\frac{R_3 + R_4}{2}\right) - R_1}{2\pi L_1 \mu_2} \quad \text{.....5.7}$$

$$\Re_2 = \Re_9$$

Then total reactance will be

$$\Re_{Total} = \Re_1 + \Re_3 + \Re_4 + \Re_5 + \Re_6 \quad \text{.....5.8}$$

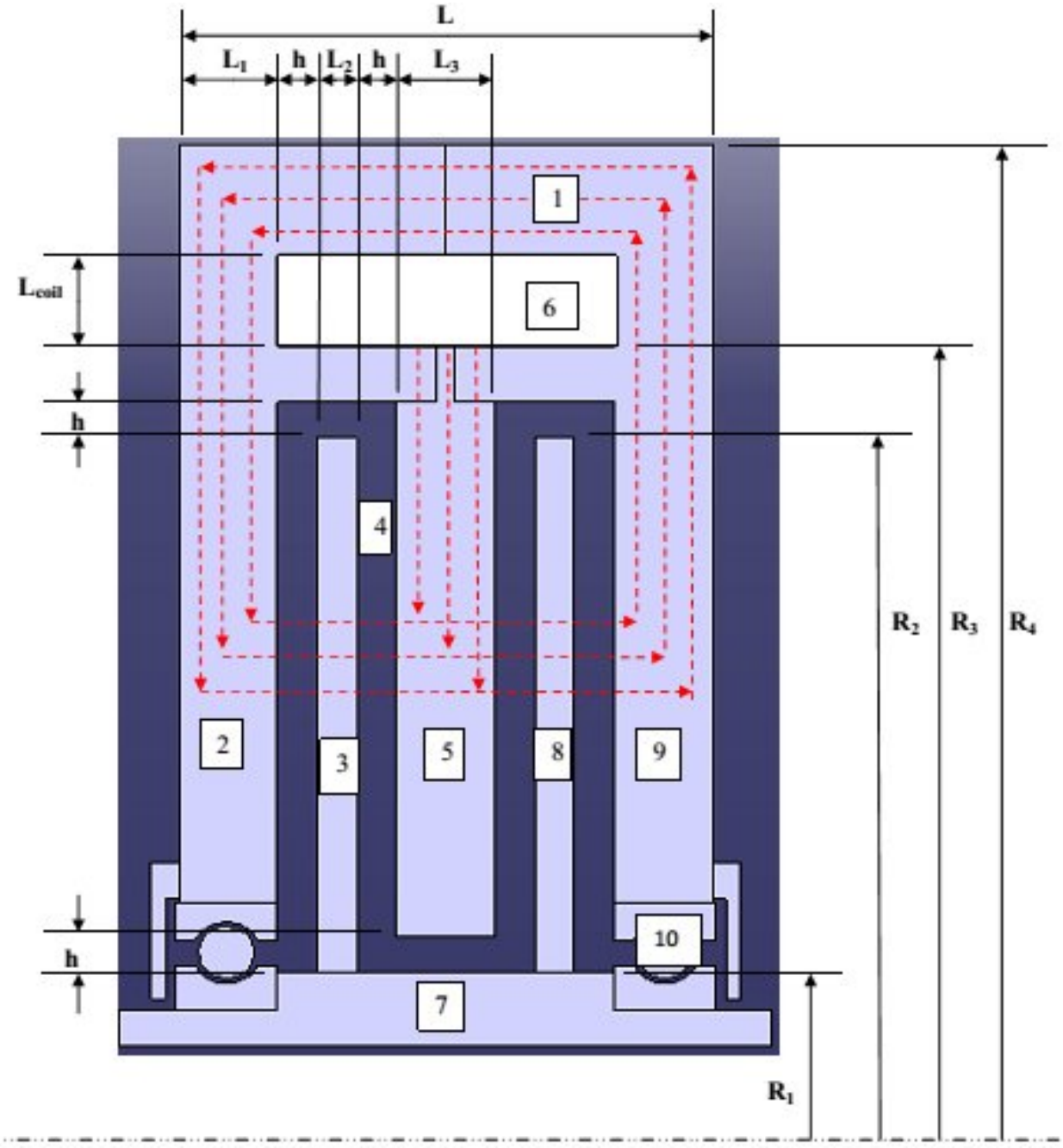

Figure 14 Double disk type magnetorheological fluid magnetic circuit diagrams

1: outer race 2: left shell 3: left shear disc 4: magnetorheological fluid 5: intermediate disc 6: excitation coil 7: rotating shaft 8: right shear disc 9: right shell 10: bearing

In this work the MR actuator installed on axle for each wheel therefore its overall dimensions must be restricted so that the brake outer diameter must be less than wheel diameter. Considering wheel size against figure 14, the maximum acceptable MRB radius for a 330mm and assume radius wheel is about $R_4 = 0.275$m, magnetorheological fluid effective outer radius is $R_2 =$ 0.195m, rotating shaft diameter $R_1 = 0.05$m and $R_3 = 0.22$m.

As for the shear disk, because its section is the same as magnetorheological fluid and magnetic saturation intensity is bigger than magnetorheological fluid's is acceptable, if slightly thicker than magnetorheological fluid's. We assume magnetorheological fluid thickness h=0.01m is selected and considering the strength requirement of left and right shell, its thickness is selected as L_1=0.025m and thickness of the shear disk L_2=0.025m finally chooses thickness of intermediate disc L_3=0.025m

Table 9 Optimum design parameters

Parameter	Optimum Value(m)
R_1	0.05
R_2	0.195
R_3	0.22
R_4	0.275
L_1	0.025
L_2	0.025
L_3	0.025
L	0.135
h	0.01
L_{Coile}	0.025

Substituting the dimensions to formula 5.4, 5.5, 5.6, 5.7, 5.8 we get reluctance of each part $\Re_3 = \Re_8 = 89.13$ $\Re_1 = 2232.6$, $\Re_4 = 35651.37$, $\Re_2 = \Re_9 = 1250.68$ therefore, the total reluctance is $\Re_{Total} = 40563.6$

However, since the magnetic fluxes in the gap (ϕ_{gap}) and in the core (ϕ_{core}) are different, the magnetic fluxes cannot be directly calculated (see Eq5.1) as the ratio between the mmf and the total reluctance of the magnetic circuit. According to [4] [12] note that magnetic flux can be written in terms of magnetic flux density B

$$\phi = \int_A BndA = \int_A \mu_r \mu_o H.ndA \quad \text{.....5.9}$$

If A is constant over the whole magnetic circuit and since ϕ remains constant, B is also assumed constant. Eq. 5.12 becomes:

$$\phi = BA \quad \text{.....5.10}$$

If we apply Ampere's law to figure 14, along the path in the center of the magnetic core, we obtain:

$$ni = \oint H.dl \quad \text{.....5.11}$$

Where l is the length of the magnetic path Eq. (5.11) can be rewritten

$$ni = \oint H_{MRF} dl_{MRF} + \oint H_{CORE} dl_{CORE} + \oint H_{DISK} dl_{DISK} \quad \text{.....5.12}$$

From the B-H relationship, H is also constant over the whole circuit and Eq. 5.12 becomes:

$$ni = \mathrm{H}_{MRF} l_{MRF} + \mathrm{H}_{CORE} l_{CORE} + \mathrm{H}_{DISK} l_{DISK} \quad \text{.....5.13}$$

Where H_{CORE}, H_{DISK} and H_{MRF} are the magnitudes of field intensity generated in the magnet core, shear disk and MR fluid respectively l_{CORE}, l_{DISK} and l_{MRF} are the length/thickness of the corresponding members.

$$B = \mu_r \mu_o H \quad \text{.....5.14}$$

Where B is magnetic flux density, Substitute Eq 5.14 in to Eq 5.13 and we get

$$ni = \frac{B_{MRF} l_{MRF}}{\mu_{rMRF} \mu_o} + \frac{B_{CORE} l_{CORE}}{\mu_{rCORE} \mu_o} + \frac{B_{DISK} l_{DISK}}{\mu_{rDISK} \mu_o} \quad \text{.....5.15}$$

From section 5.4.1(figure 11)B-H curve saturation flux density of low carbon steel, AISI 1018 is B_A=2.4T and relative permeability $\mu_{rA} = 800$ and from figure 12 B-H curve a saturation flux density of MRF-132DG B_H is 1.6T and relative permeability $\mu_{rH} = 8$. The circuit length of a core, shear disk and MR fluid, (see table 9) $l_{CORE} = 0.535\text{m}$, and from $l_2 = 0.025\text{m}$ and $h = 0.01\text{m}$

To determine necessary generating magnetomotive force or mmf in amp-turns (ni) substitute Eq 5.15

$$ni = \frac{1.6 \times 0.01}{8 \times 4\pi \times 10^{-7}} + \frac{2.4 \times 0.535}{800 \times 4\pi \times 10^{-7}} + \frac{2.4 \times 0.025}{800 \times 4\pi \times 10^{-7}}$$

$$ni = 2928.7\text{A.turn}$$

According to this study, the most efficient wire size in this work is the AWG 17 size copper wire is used to wind the coil of the MRB's electromagnet. From appendix B maximum current is 2.9A, area 1.04[mm^2], diameter 1.15062[mm]

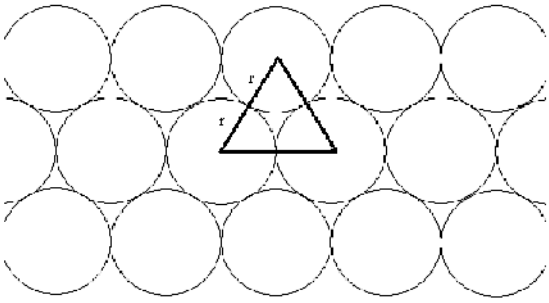

Figure 15 Wire configurations in a coil [4]

In order to maximize the amount of applied current density, the dimensional space where the coil is located needs to be optimized along with the other dimensional parameters. In addition, a wire size, with the highest current density capacity was selected. In order to find the most efficient wire in terms of the current density carrying capacity, a coil with a winding configuration of figure 15 was studied. By drawing an equilateral triangle, the effective cross sectional area of the wire can be calculated within the triangular area and the corresponding current density application capacity was calculated by dividing the mmf by the calculated triangular area [4].

To calculated the effective cross sectional area of the wire [4]

$$A = \frac{1}{2} \times 2r \times 2r \sin 60 \quad \text{.....5.15}$$

$$A = 0.5733 \text{mm}^2$$

The current density carrying capacity of a coil is

$$I_{densty} = \frac{ni}{A} \quad \text{.....5.16}$$

$$I_{densty} = 5494.7 \text{A turn/mm}^2$$

To calculate H_{MRF}, B_H=1.6T, relative permeability $\mu_{rMRF} = 8$, μ_o is vacuum's permeability (i.e. $\mu_0 = 4\pi 10^{-7}$H/m) substitute in Eq 5.14

$$H_{MRF} = \frac{B_H}{\mu_{rMRF}\mu_o} = 159154.9 \, A/m$$

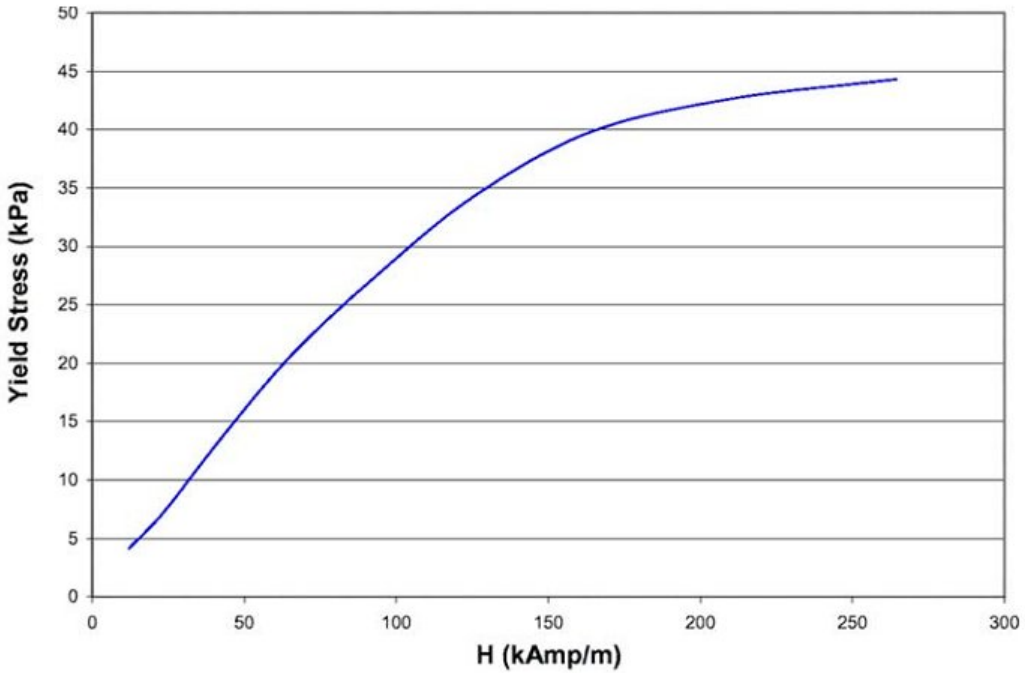

Figure 16 yield stress versus magnetic field intensity for MRF-132DG [1]

5.5 Centrifugal force acting on MR brake

When two shear disk rotate in MRF the centrifugal load the pressure/stress is applied to the surface of the brake surface which is dependent on the mass of the disc, rotational speed of the disc and the radius of the rotating disc.

the rotational speed of the rotating disc is calculated from the speed of the vehicle in relation to the radius of the rotating disc . The rotating disc with radiuses of 0.195m therefore the rotational speed of rotating disc calculated as follow

$$\omega = \frac{22.2}{0.195} = 113.8 rad/s$$

Centrifugal force on the rotating disc is expressed as

$$F_C = \rho_{disc} \omega^2 R_2 \quad \text{.....5.18}$$

Where F_c is the centrifugal force, from table 6 ρ_{disc} is density of rotating disc is $8030 Kg/m^2$. Then the centrifugal load of the rotating disc is about

$$F_C = 8030 \times 113.8^2 \times 0.195$$

$$F_C = 20.3 \times 10^6 N$$

5.6 The maximum braking torque generated by MR brake

In this paper the MR actuator has two the shear disk N is 4, and from table 8 η is 0.25Pa s and from section 3.1 the angular speed of shear disk is113.8 rad/s, from table 9, R_1 is 0.05m, R_2 is 0.195m and magnetorheological fluid gap h is 0.01m

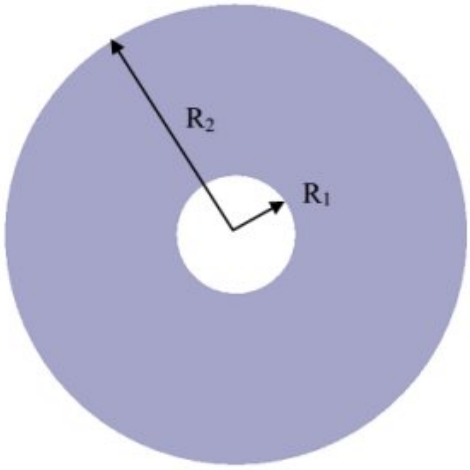

Figure 17 shear disk analytical diagram

From chapter 4, Eq 4.9 torques generated due to the viscosity of the fluid is given. Substitute the values and we get

$$T_\eta = \frac{\pi}{2\times 0.01}\times 4\times 0.25\times 113.8\times\left(0.195^4 - 0.05^4\right)$$

$$T_\eta = 25.7Nm$$

To calculate braking torque generated due to the applied magnetic field see chapter 4 Eq 4.11, from table 8 we get K=0.269, β =1 and from section 5.4.2 the magnetic field intensity of magnetorheological fluid is 159154.9A/m substitute the values and we get

$$T_H = \frac{2\pi}{3}\times 4\times 0.269\times 159154.9^1\times\left(0.195^3 - 0.05^3\right)$$

$$T_H = 2.6\times 10^3\, Nm$$

Finally total braking torque generated by brake is sum of torque generated due to the applied magnetic field and torques generated due to the viscosity of the fluid

$$T_b = 2.6\times 10^3 + 25.7$$

$$T_b = 2.6\times 10^3\, Nm$$

5.7 Thermal Analysis

In a braking system, the kinetic energy of rail vehicle is transformed into a heat energy therefore highest heat energy we expect from highest speed. This energy is characterized by a total heating of the MRB. The heat energy during braking over the flat track on each wheel can be calculated using this equation from the kinetic energy.

I. The initial kinetic energy imposed in to the tramcar is given by the sum total of translational and rotational.

$$KE = \frac{1}{2} m_v v_o^{\,2} + \frac{1}{2} \mathrm{I} \omega_o^{\,2} \quad \text{.....5.17}$$

In most analysis the contribution of the rotating masses of the wheel set and brake is taken to be 10% the tare weight of the axle load of the train.

$$KE = \frac{1}{2}(1.1) m_v v_o^{\,2} \quad \text{.....5.18}$$

Where

m_v Total mass of the vehicle

v_o Initial speed of the train

From table 4, $m_v = 64000\,Kg$ and $v_o = 22.2\,m/s$

$$KE = \frac{1}{2}(1.1) \times 64000 \times 22.2^2$$

$$KE = 31.54 \times 10^6\,J$$

Assume the heat energy during braking over the flat track and 52% of KE is converted to heat because the proposed MRB configuration generate 52% of require braking torque cannot able to stop a vehicle.

$$0.52 \times KE = Q \quad \text{.....5.19}$$

Where Q is heat energy developed due to the kinetic energy of the train is equal to total of kinetic energy imposed in to the tramcar

$$0.52KE = Q = 16.4 \times 10^6 J$$

II. Area of the contacting faces with magnetorheological fluid (see figure17)

$$A = 4\pi\left(R_2{}^2 - R_1{}^2\right) \quad \text{.....5.20}$$

From table 9 $R_1 = 0.05m$ and $R_2 = 0.195m$

$$A = 4\pi\left(0.195^2 - 0.05^2\right)$$

$$A = 0.4464m^2$$

III. The total heat flux is given by

$$\dot{q} = \frac{Q}{A \times t_b} \quad \text{.....5.21}$$

Where

Q total heat energy developed due to the kinetic energy

A is contact area

t_b is braking time

$$\dot{q} = \frac{16.4 \times 10^6}{0.4464 \times 14.8}$$

$$\dot{q} = 2{,}482{,}321.1 w/m^2$$

The analysis is done by taking the distribution of braking torque between the front and rear axle is 70:30

Heat flux on each front wheel MRB is given

$$\dot{q} = \frac{2482321.1 \times 0.7}{2}$$

$$\dot{q} = 869 \times 10^3 \, w/m^2$$

5.7.1 Heat convection coefficient

To calculate the convective film coefficient between outer brake surface and air as a function of the railway vehicle velocity, the following formula should be used

$$h = \frac{0.037 \times K_{air}}{2R_b} \mathrm{Re}^{0.8} \times \mathrm{Pr}^{0.33} \quad \text{.....5.22}$$

Bur the Reynolds number Re and Prandtl number Pr are given as the following formula

$$\mathrm{Re} = \frac{2\rho_{air} \times V_{rail} \times R_b}{\mu_{air}} \quad \text{.....5.23}$$

$$\mathrm{Pr} = \frac{C_{air}\mu_{air}}{K_{air}} \quad \text{.....5.24}$$

Where

h= Heat convection coefficient

K_{air}= Conductivity of air (0.0241 w/mK)

V_{rail}= Railway speed

μ_{air} = dynamic viscosity of air (12.34×10^{-6} m^2/s)

C_{air}= specific heat capacity of air

From specification railway speed is 22.2 m/s and radius of a brake R_b is 0.275m, Reynolds numbers became

$$\mathrm{Re} = \frac{2\times1.184\times0.275\times22.2}{12.34\times10^{-6}}$$

$$\mathrm{Re} = 1.1715\times10^{6}$$

Prandtl number is calculated as follow

$$\mathrm{Pr} = \frac{1009\times12.34\times10^{-6}}{0.0241}$$

$$\mathrm{Pr} = 0.517$$

Finally heat convection coefficient is became

$$h = \frac{0.037\times0.0241}{2\times0.275}\times\left(1.1715\times10^{6}\right)^{0.8}\times\left(0.517\right)^{0.33}$$

$$h = 110\, w/m^2\,{}^{\circ}c$$

5.8 MR brake 3D CAD modal

Magnetorheological brake a 3-D CAD model was generated using software called CATIA

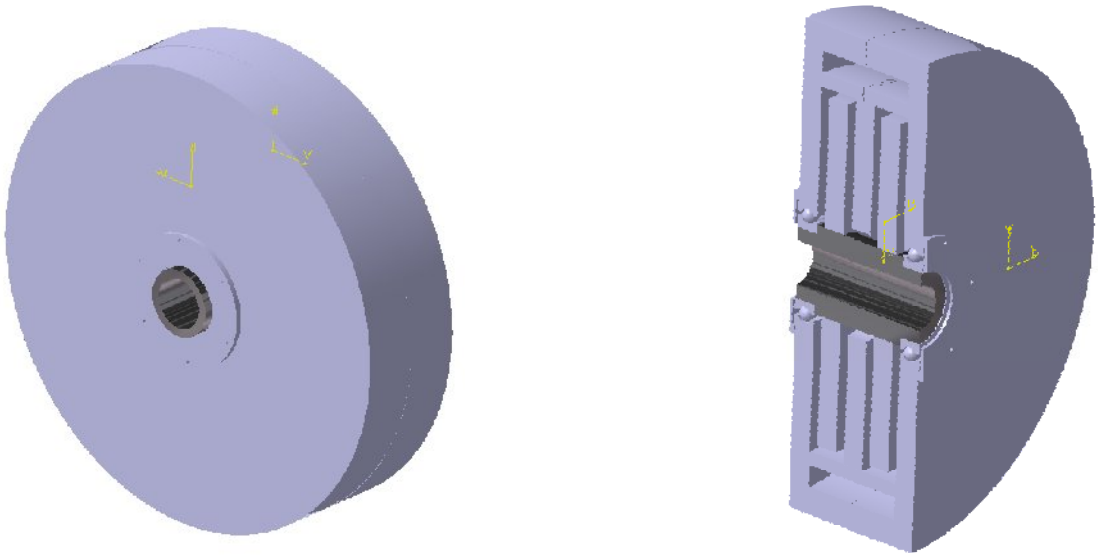

A: pictorial view B: section view

Figure 18 MR Brake 3D CAD modal:

CHAPTER SIX

6 FINITE ELEMENT ANALYSIS

Most numerical approaches on MR brakes preset a braking time or deceleration rate, for analyzing the process of braking; it is very useful to use FEM simulations based on the adopted analytical model for defining heat sources at surfaces which are in contact with shear disc.
This study will use the FEA software ANSYS14 version to carry out steady state thermal analysis and the thermo - mechanical stresses of Magnetorheological brake a during braking conditions will be determined.

6.1 Introduction to Finite Element Analysis

Finite element method is a numerical procedure that can be used to obtain solution to a large class of engineering problem involving stress analysis, heat transfer, electromagnetism and fluid flow problem may be analyzed with finite element method. In practice, a finite element analysis usually consists of three principal steps.

Preprocessing:

- Create and discretize the solution domain into finite elements ;that is subdivide the problem into nodes and elements
- Assume a shape function to represent the physical behavior of an element ;that is an approximate continuous function is assumed to represent the solution of an element
- Develop equation for an element
- Assemble the element to present the entire problem construct the global stiffness matrix
- Apply boundary condition initial condition and loading

Solution phase

- Solve a set of linear or nonlinear algebraic equation simltionusly to obtain nodal values such as displacement value at different nodes or temperature values at different nodes in heat transfer problem.

Post processing phase

- Obtain other important information .at this point you may be interested in values of principal stresses, heat fluxes etc

6.2 Introduction to FEA Software ANSYS

ANSYS is comprehensive general purpose finite element computer programming. ANSYS is capable of performing static, dynamic, heat transfer, fluid flow and electromagnetism analysis.

6.2.1 General Analysis Procedure in ANSYS

Similar to solving problems analytically, it needs to define: the solution domain, the physical the model, the boundary conditions and the physical properties.

- Geometrical Definition:
- Model Generation
- Define Material Properties
- Generate Mesh
- Finite element generation
- Boundary conditions and loading
- Solution
- Post-Processor

6.3 Assumptions

- The analysis is done taking the distribution of the braking torque between the front and rear axle is 70:30
- Brakes are applied on all the eight wheels
- The specific heat of the material used is constant throughout and does not change with the temperature.
- The heat energy during braking over the flat track
- The shear stress, τ_y is constant over the active MR area.
- Uniformly distributed load the height of the center of gravity is half of height of tramcar

6.4 Transient thermal analysis using ANSYS 14

The analysis is carried out for three dimensional solid of the MRB. In the zone of temporary contact of the MRF and shear disc, the thermal flux is assigned, which differs in the area of disc at any instant of braking time corresponding to the components of the intensity of heat flux product .The numerical modeling of thermal effects was performed according to the following assumptions in ANSYS 14 work bench module.

6.4.1 Geometrical model

In the three-dimensional model of solid MRB its symmetry there for half section of solid MRB is used for this analysis

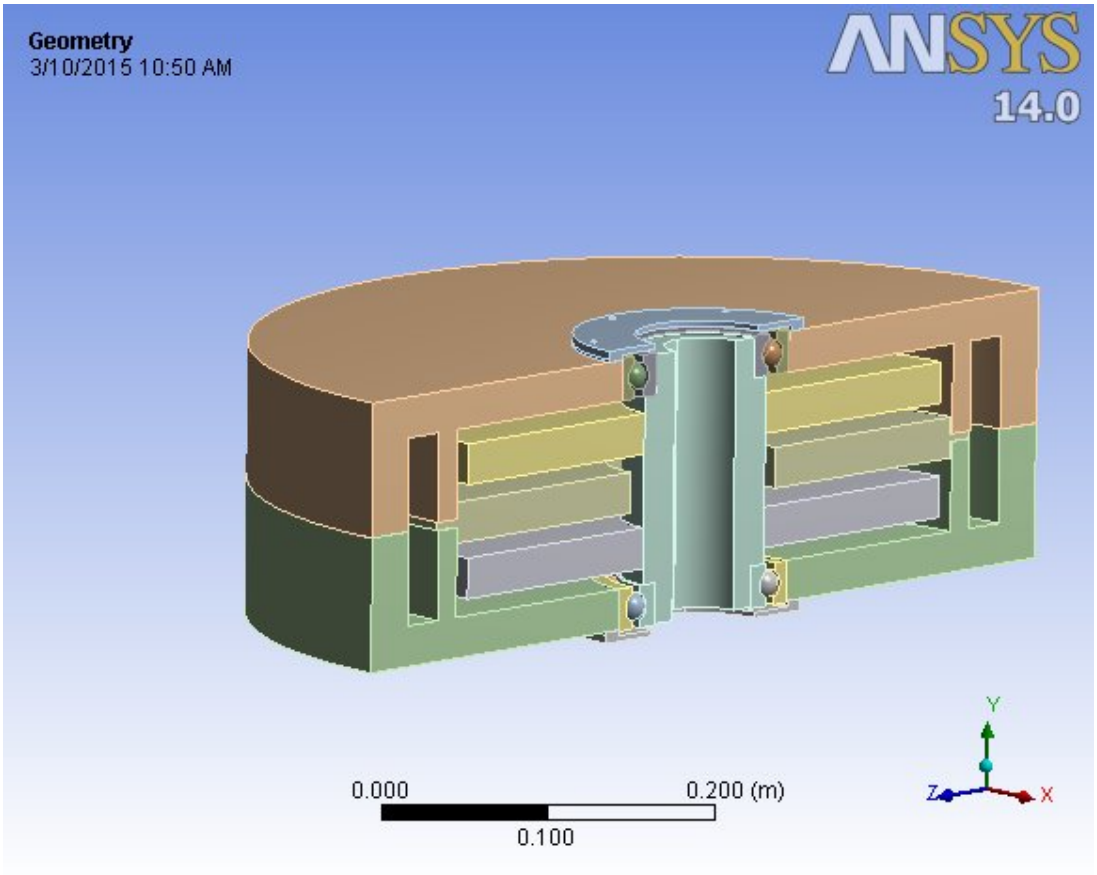

Figure 19 Geometric Models of MRB

6.4.2 Definition of Material

Table 10 Material Properties of MRB [4]

Property	Value
Tensile Strength(MPa)	634
Yield Strength(MPa)	386
Hardness Rockwell B	197
Density(Kg/m^3)	8030
Modulus of Elasticity(GPa)	210
Thermal Conductivity (W/m-K)	51.9
Specific Heat(J/Kg-K)	486

6.4.3 Meshing

Meshing is discretizing the solid object to finest parts to perform the analysis to get the precise value at each and every elements of the meshed object. For this analysis, patch conforming method were used and the output of the mesh consists of 45300 nodes and 22820 tetrahedral elements.

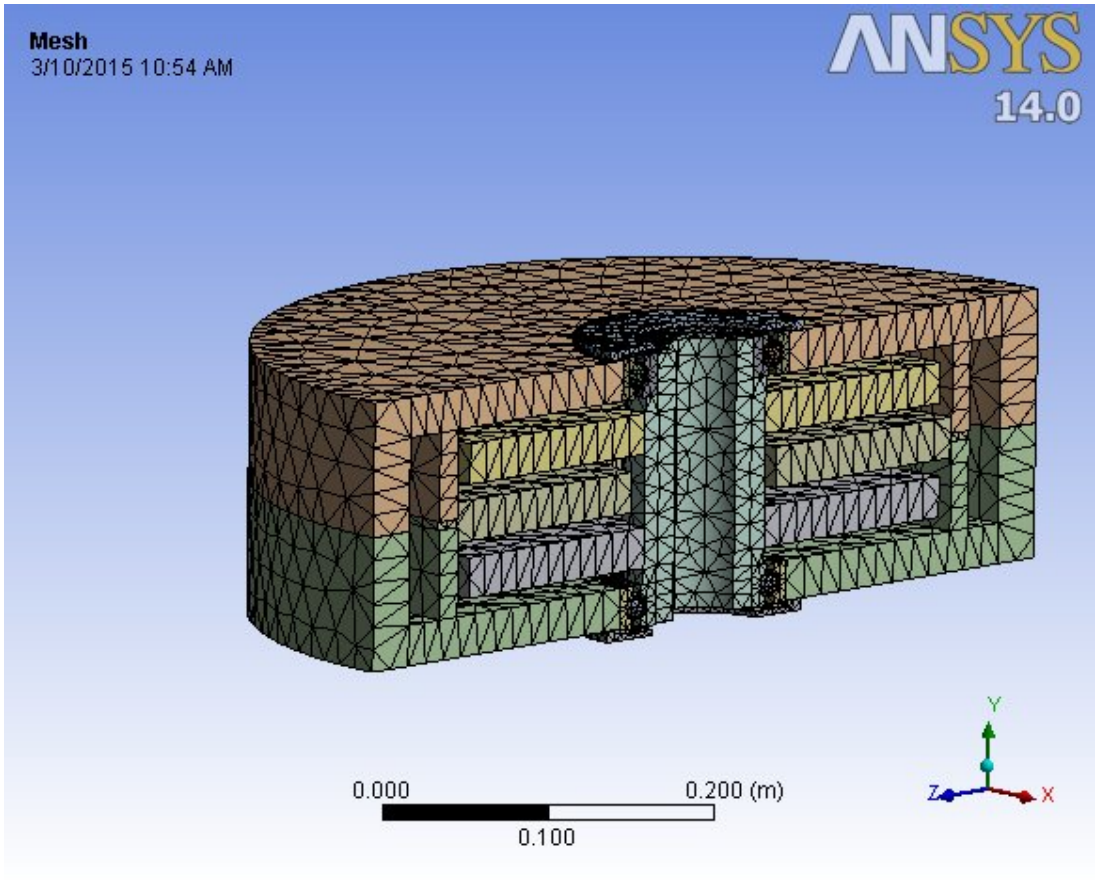

Figure 20 Meshed model of MRB

6.4.4 Definition of the loads and boundary conditions

After completion of the finite element model, it was necessary to apply constraints and loads to the model. The analyzed MRB brake is subjected to the following loads.

Table 11 Input data for transient thermal analysis

Input	Value
Initial temperature	$25°c$
Maximum heat flux	$869\times10^{3}\ w/m^{2}$
film coefficient between outer brake surface and air	$110\ w/m^{2}\ °c$

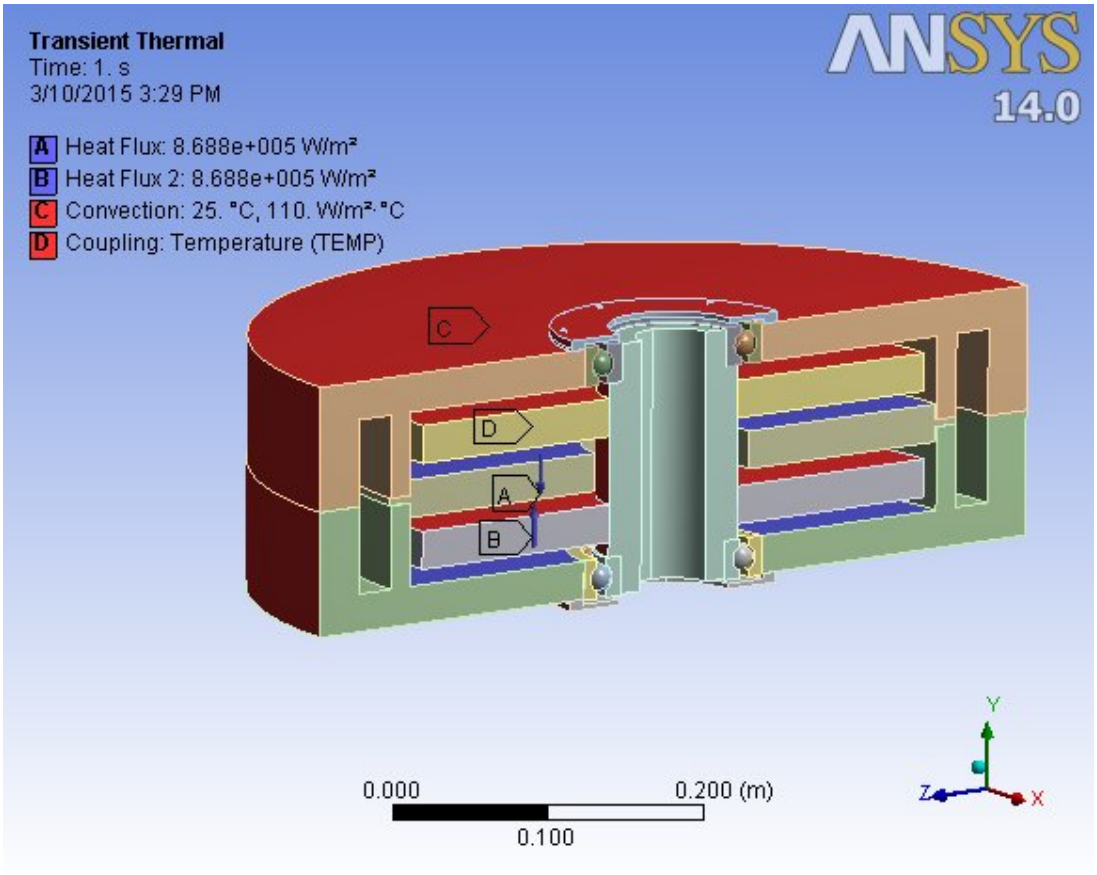

Figure 21 the loads and boundary conditions for thermal analysis

6.5 Static structural analysis using ANSYS 14

The braking process uses friction between the solidified MRF and rotating disc (shear disc) to decreases of the speed moving railway vehicle by transforming kinetic energy into heat. This heat induces stresses in the brake. Therefore, thermo-mechanical stress analysis of MR brake is important to understand the behavior of the brake while in operation.

Two steps are required for solving the ANSYS analysis for thermo-mechanical stress analysis. The first is to solve the temperature rise over the brake and the second is couple thermal analysis to the structural analysis of the brake.

6.5.1 Definition of the loads and boundary conditions

After completion of the finite element model, it was necessary to apply constraints and loads to the model. The analyzed MRB brake is subjected to the following loads.

Table 12 input data for Structural analysis

Input	Value
Initial temperature	$25°c$
Centrifugal force	$20.3\times10^{6}\,N$
Rotational speed	$113.8\,rad/s$
Gravitational acceleration	$9.81\,m/s^{2}$
Pressure due to shear stress develop by MRF	$40\times10^{3}\,Pa$

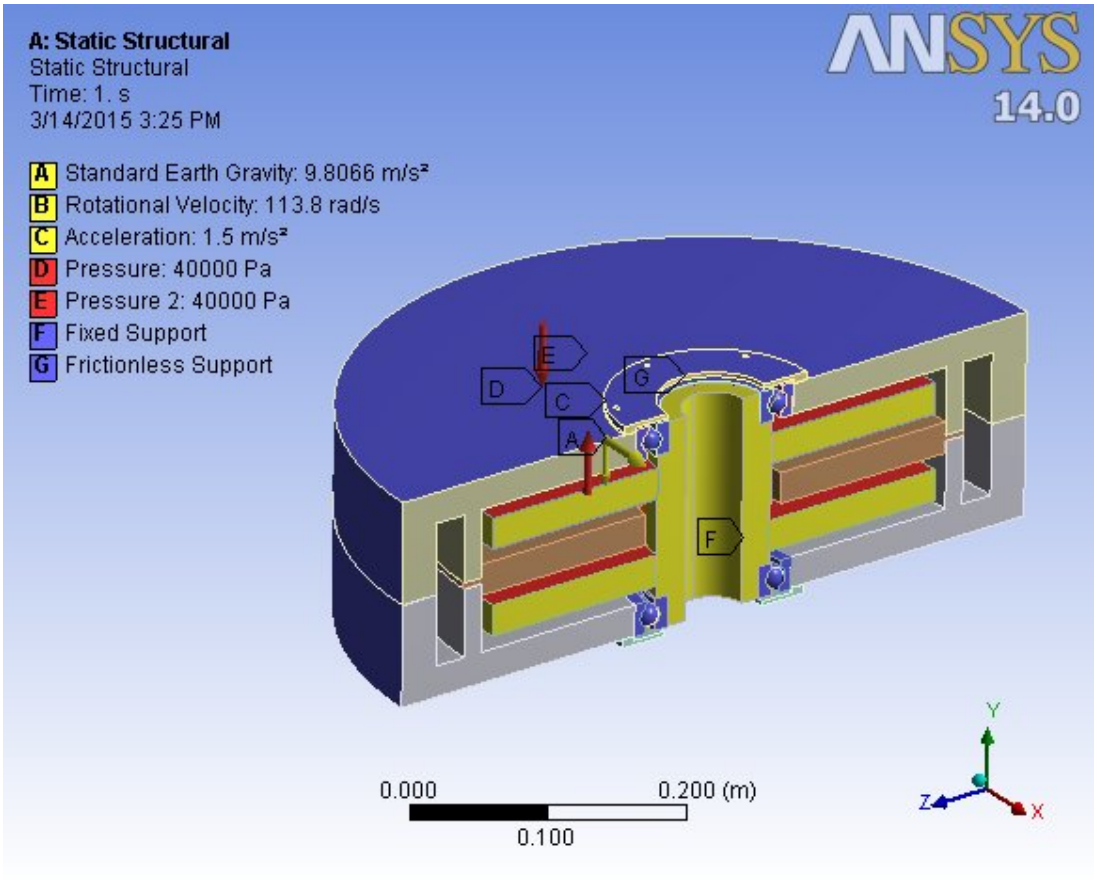

Figure 22 the loads and boundary conditions for structural analysis

CHAPTER SEVEN

7 RESULTS AND DISCUSSIONS

Due to the application of brakes on brake heat generation takes place due to friction and this temperature so generated has to be conducted away and dispersed across the brake cross section. The condition of braking is very severe and thus thermal analysis is carried out and with the above load structural analysis is also performed for analyzing the stability of the structure. The thermal and structural results obtained from ANSYS are deformation; Von Mises stress and temperature gradient.

7.1 Transient thermal Analysis Result

According to the transient thermal analysis result the maximum temperature rises by almost 369.78^{o}C (fig. 23). In addition, the result showed that the operating temperature can intermittently reach outside the recommended temperature range of the MR fluid. There for MRB modal need effective passive or active cooling mechanism.

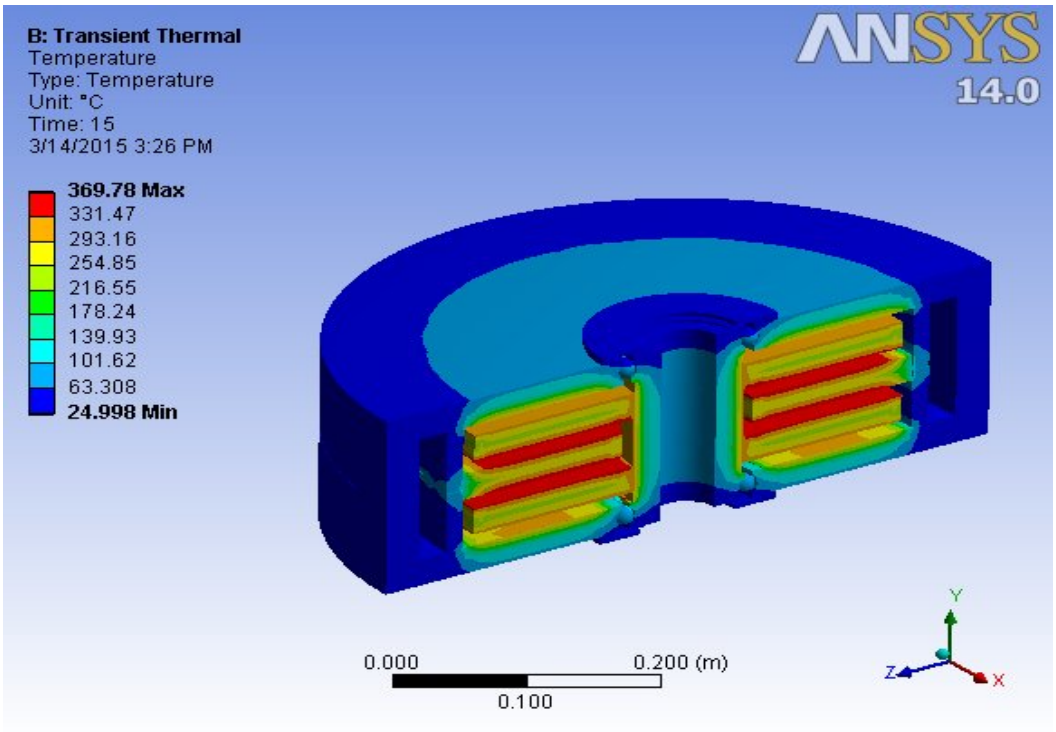

Figure 23 Temperature gradients on MRB

7.2 Static structural Analysis Result

7.2.1 Total deformation

According to the analysis result the maximum and the minimum resulting deformation are $3.5292\times10^{-5}\,m$ and 0 therefore the brake operate safely with slight deformation.

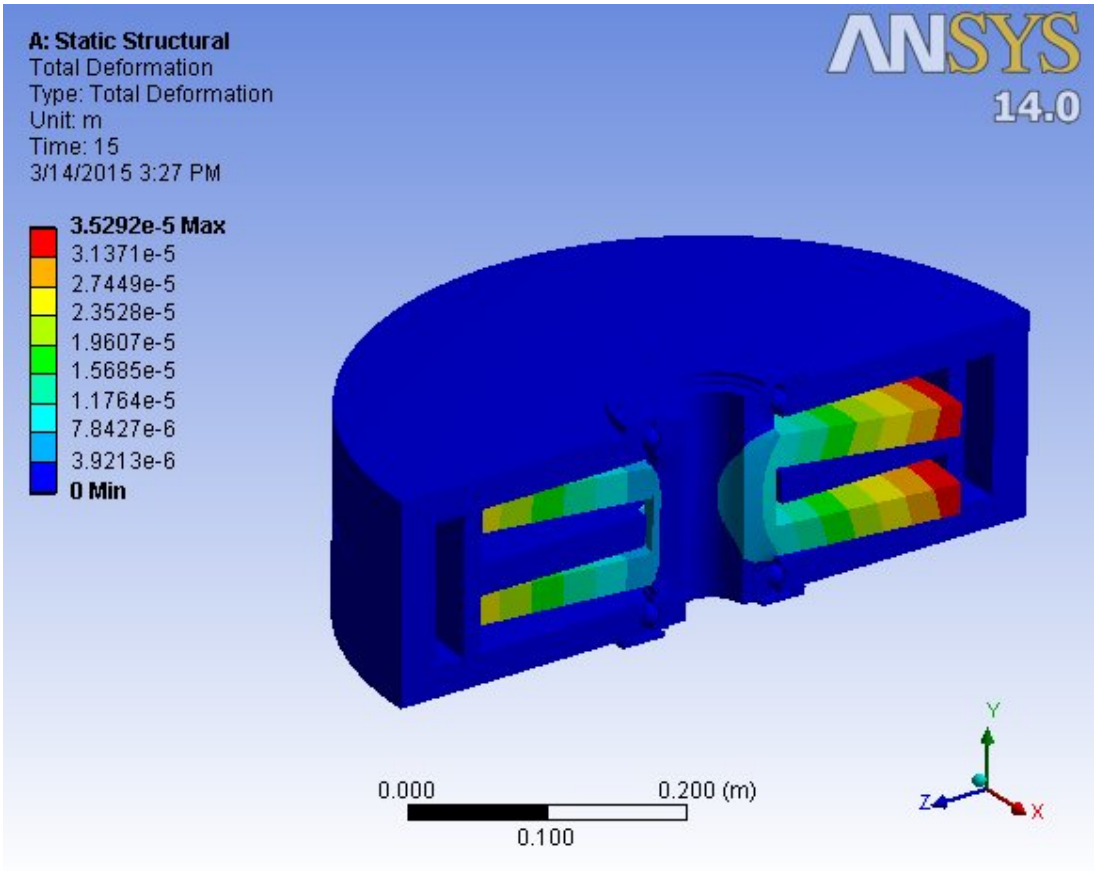

Figure 24 Total deformations on the MR Brake

7.1.2 Von Mises Stress

From the output result of the analysis the maximum equivalent (Von messes when the train starts braking is and the minimum equivalent (Von messes) stress induced on the brake is 1.1109×10^{8} and 0.61451 Pa when we compare to material yield strength with safety factor of 3.4 there for the brake withstand thermo mechanical stress which is applied on it.

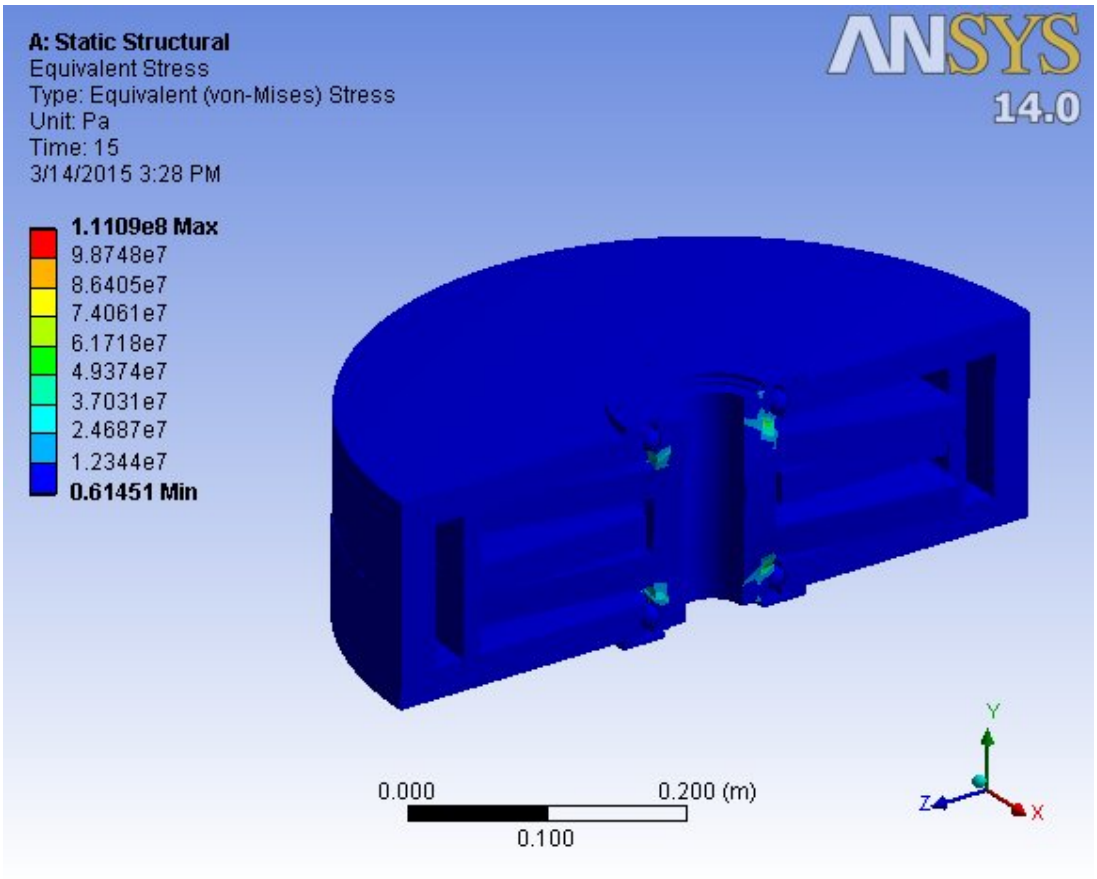

Figure 25 Von Mises Stress

7.3 Braking torque generated by MR brake and braking torque required to stop rail vehicles

Note that in order to stop a light rail vehicle with a deceleration of 1.5 m/s^2 each brake on wheel has to be generating over 4368.15Nm braking torque (see section 3.3). The MRB can generate only 2600Nm (section 5.6) braking torque, so that MRB configuration cannot supply enough braking torque to stop a light rail vehicle. In order to further increase the braking torque a number of improvements can be made:

1) Multidisciplinary design optimization to maximize the braking torque and minimize the weight of the MRB with additional disks is shown for the same design configuration proposed in this work.
2) Another way of increasing the braking torque generation is to change the basic magnetic circuit configuration.

With a combination of these improvements, there is a potential to further increase the braking torque capacity of an MRB

CHAPTER EIGHT

8 CONCLUSION AND RECOMMENDATION

Based on a commercially available magnetorheological fluid, a new brake system was proposed to light rail vehicle. The mathematical model of the proposed MRB was presented, and a 3-D CAD model of the optimum MRB design was then generated in order to conduct a 3-D finite element analyses of the MRB was created and mechanical analyses and heat transfer phenomena within the system .

One of the major concerns with the actual implementation of an MRB into a light rail vehicle is the high temperature effect on the MR fluid. In practice, the proposed MRB would likely require a physical (e.g. active or passive) cooling system to alleviate the heating problem in the MR fluid and thus improving the braking performance. Since, the brake actuator transforms kinetic energy into heat; all kinetic energy of the rail vehicle will be converted into heat in the MRB. As mentioned previously in the material selection section (Sec. 5.2) of this thesis, the magnetic properties are highly dependent on the temperature of the MR fluid (the viscosity varies with temperature). Due to this reason, I recommend active or passive cooling system has to be included or the structural design has to be changed to improve heat dissipation capabilities, unless a MR fluid with better temperature properties becomes available. In addition, this work showed that the proposed MRB configuration cannot supply enough braking torque to stop a vehicle. Therefore, the braking capacity of the MRB must be improved by MRB will be designed with an increased number of disks and a modified magnetic circuit configuration. Additional pointes which is consider as future where

- the study of the reduction of motion resistance due to the viscosity of MR fluid under normal operation,
- Build a working prototype to verify the performances.

9 REFERENCE

[1] Edward J Park, Dilian Stoikov, Luis Falcao da Luz, Afzal Suleman, "A performance evaluation of an Automotive magnetorheological brake design with a sliding mode controller", Victoria, BC, Canada: University of Victoria; Received 14 March 2006.

[2] Edward J Park, Luis Falca˜o da Luz, Afzal Suleman, "Multidisciplinary design optimization of an automotive magnetorheological brake design" Victoria, BC, Canada: University of Victoria; 2007.

[3] Kerem Karakoc, Edward J Park, Afzal Suleman, "Design considerations for an automotive magnetorheological brake", Victoria, BC, Canada: University of Victoria; 2008.

[4] Kerem Karakoc, "Design of a Magnetorheological Brake System Based on Magnetic Circuit Optimization", MASc thesis. Turkey: BSc - Bogazici University, 2005.

[5] Roger Johansson, "A fault tolerant architecture for brake-by-wire in railway cars" Göteborg, Sweden: Chalmers Lindholmen University College; 2003.

[6] M. Kciuk, R. Turczyn, "Properties and application of magnetorheological fluids" journal of Achievements in Materials and Manufacturing Engineering, AMME, vol.18, 2006, issue 1-2.

[7] Tran Dinh Huy, Nguyen Quoc Hung, Tran Cong Hung, "optimization and design of a single disk-type MR brake" Vietnam, Hochiminh City University of Technology (HUTECH), 2010.

[8] Mukund A.Patil, Ashutosh S.Zare, "Theoretical Studies on Magnetorheological Fluid Brake" G. H. Raisoni Institute of Engineering and Management, Jalgaon,2012.

[9] Thomas D.Gillespie "Fundamentals of vehicle dynamics"

[10] Luo Yiping, Xu Biao, Ren Hongjuan, Chen Fuzhi," Design of magnetorheological fluid dynamometer which electric current and resisting moment have corresponding relationship" College of Automobile Engineering, Shanghai University of Engineering Science, Shanghai, China, Vol. 2, No. 2, 2014.

[11] Ahmad Zaifazlin. Zainordin, Mohd, Azman Abdullah and Khisbullah. Hudha, "Experimental Evaluations on Braking Responses of Magnetorheological Brake" International Journal of Mining, Metallurgy & Mechanical Engineering (IJMMME) Volume 1, Issue 3 (2013)

[12] More Thomas Avraam," MR-fluid brake design and its application to a portable muscular rehabilitation device", Thesis submitted in candidature for the degree of Doctor in Engineering Sciences, Universite Libre de Bruxelles,November 2009.

[13] S A Mazlan, N B Ekreem and A G Olabi," Apparent stress-strain relationships in experimental equipment where magnetorheological fluids operate under compression mode" School of Mechanical and Manufacturing Engineering ,Dublin City University, Glasnevin, Dublin 9, Ireland

[14] Quoc-Hung Nguyen and Seung-Bok Choi,"Optimal design methodology of magnetorheological fluid based mechanisms".

[15] Lord Materials Division," Magnetic circuit design", Thomas Lord research center, 110 Lord drive, Cary, NC 27511.

[16] http://www.eng-tips.com/veiwthread.cfm

[17] Lord Materials Division," Designing with MR Fluids", Thomas Lord research center, 110 Lord Drive, Cary, NC 27511.

[18] Mr. Vinayak D. Dabade, Prof. Y. R. Patil, Prof.M.V. Kharade, Prof. P.R. Patil," Smart Material Magneto Rheological Fluid" IOSR Journal of Mechanical Engineering (IOSR-JMCE) ISSN: 2278-1684, PP: 48-52

[19] Giuseppe Marannano, Gabriele Virzi Mariotti, Cedomir Duboka" Analysis of the behaviour of an optimized magnetorheological brake" University of Belgrade, faculty of mechanical engineering; Vol. 2 Iss. 2, June 2013

[20] Mohammadhossein Hajiyan, Shohel Mahmud, and Hussein A. Abdullah," Magnetorheological fluid based braking system using L-shaped disks" School of Engineering, University of Guelph, 50 Stone Road East ,Guelph, Ontario, Canada

[21] Husain Abdulrahman Ahmad," Dynamic braking control for accurate train braking distance estimation under different operating conditions" the faculty of the Virginia Polytechnic Institute and State University in partial fulfillment of the requirements for the degree of doctor of philosophy in mechanical engineering ;Blacksburg, VA, USA February 20, 2013

APPENDIX

Appendix A: B–H Variation of Steel 1018 (Low carbon steel) [16]

Steel 1018 (Low carbon steel)

H (amp/m)	B (Tesla)
0	0
238.73	0.250
795.78	0.925
1591.55	1.250
2387.33	1.390
3978.88	1.525
7957.75	1.710
15915.5	1.870
23873.25	1.955
39788.75	2.020
79577.5	2.110
159155	2.225
318310	2.430

Appendix B: American Wire Gauge Conductor Size Table

American wire gauge (AWG) is a standardized wire gauge system for the diameters of round, solid, nonferrous, electrically conducting wire. The larger the AWG number or wire gauge, the smaller the physical size of the wire. The smallest AWG size is 40 and the largest is 0000 (4/0). AWG general rules of thumb - for every 6 gauge decrease, the wire diameter doubles and for every 3 gauge decrease, the cross sectional area doubles. Note- W&M Wire Gauge, US Steel Wire Gauge and Music Wire Gauge are different systems.

American Wire Gauge (AWG) Sizes and Properties Chart / Table

Table lists the AWG sizes for electrical cables /conductors. In addition to wire size, the table provides values load (current) carrying capacity, resistance and skin effects. The resistances and skin depth noted are for copper conductors. A detailed description of each conductor property is described below table.

AWG	Diameter [inches]	Diameter [mm]	Area [mm^2]	Resistance [Ohms / 1000 ft]	Resistance [Ohms /km]	Max Current [Amperes]	Max Frequency for 100% skin depth
0000 (4/0)	0.46	11.684	107	0.049	0.16072	302	125 Hz
000 (3/0)	0.4096	10.40384	85	0.0618	0.202704	239	160 Hz
00 (2/0)	0.3648	9.26592	67.4	0.0779	0.255512	190	200 Hz
0 (1/0)	0.3249	8.25246	53.5	0.0983	0.322424	150	250 Hz
1	0.2893	7.34822	42.4	0.1239	0.406392	119	325 Hz
2	0.2576	6.54304	33.6	0.1563	0.512664	94	410 Hz
3	0.2294	5.82676	26.7	0.197	0.64616	75	500 Hz
4	0.2043	5.18922	21.2	0.2485	0.81508	60	650 Hz
5	0.1819	4.62026	16.8	0.3133	1.027624	47	810 Hz
6	0.162	4.1148	13.3	0.3951	1.295928	37	1100 Hz
7	0.1443	3.66522	10.5	0.4982	1.634096	30	1300 Hz
8	0.1285	3.2639	8.37	0.6282	2.060496	24	1650 Hz
9	0.1144	2.90576	6.63	0.7921	2.598088	19	2050 Hz

10	0.1019	2.58826	5.26	0.9989	3.276392	15	2600 Hz
11	0.0907	2.30378	4.17	1.26	4.1328	19	2050 Hz
12	0.0808	2.05232	3.31	1.588	5.20864	15	2600 Hz
13	0.072	1.8288	2.62	2.003	6.56984	12	3200 Hz
14	0.0641	1.62814	2.08	2.525	8.282	9.3	4150 Hz
15	0.0571	1.45034	1.65	3.184	10.44352	7.4	5300 Hz
16	0.0508	1.29032	1.31	4.016	13.17248	5.9	6700 Hz
17	0.0453	1.15062	1.04	5.064	16.60992	2.9	13 k Hz
18	0.0403	1.02362	0.823	6.385	20.9428	2.3	17 kHz
19	0.0359	0.91186	0.653	8.051	26.40728	1.8	21 kHz
20	0.032	0.8128	0.518	10.15	33.292	1.5	27 kHz
21	0.0285	0.7239	0.41	12.8	41.984	1.2	33 kHz
22	0.0254	0.64516	0.326	16.14	52.9392	0.92	42 kHz

Table 1: American Wire Gauge (AWG) Cable / Conductor Sizes and Properties

AWG Notes: American Wire Gauge (AWG) is a standardized wire gauge system used predominantly in the United States to note the diameter of electrically conducting wire. The general rule of thumb is for every 6 gauge decrease the wire diameter doubles and every 3 gauge decrease doubles the cross sectional area.

Diameter Notes: A mil is a unit of length equal to 0.001 inch (a "milli-inch" or a "thousandth of one inch") i.e. 1 mil = 0.001".

Resistance Notes: The resistance noted in the table above is for copper wire conductor. For a given current, you can use the noted resistance and apply Ohms Law to calculate the voltage drop across the conductor.

Current (ampacity) Notes: The current ratings shown in the table are for power transmission and have been determined using the rule of 1 amp per 700 circular mils, which is a very conservative rating. For reference, the National Electrical Code (NEC) notes the following ampacity for copper wire at 30 Celsius:

14 AWG - maximum of 20 Amps in free air, maximum of15 Amps as part of a 3 conductor cable;

12 AWG - maximum of 25 Amps in free air, maximum of20 Amps as part of a 3 conductor cable;

10 AWG - maximum of 40 Amps in free air, maximum of30 Amps as part of a 3 conductor cable.

Check your local electrical code for the correct current capacity (ampacity) for mains and in wall wiring.

Skin Effect and Skin Depth Notes: Skin effect is the tendency of an alternating electric current (AC) to distribute itself within a conductor so that the current density near the surface of the conductor is greater than that at its core. That is, the electric current tends to flow at the "skin" of the conductor. The skin effect causes the effective resistance of the conductor to increase with the frequency of the current. The maximum frequency show is for 100% skin depth (i.e. no skin effects).